IKKβ links vascular inflammation to obesity and atherosclerosis

Yipeng Sui,[1] Se-Hyung Park,[1] Jinxian Xu,[1] Sébastien Monette,[3]
Robert N. Helsley,[1] Seong-Su Han,[4] and Changcheng Zhou[1,2]

[1]Graduate Center for Nutritional Sciences, [2]Saha Cardiovascular Research Center, University of Kentucky, Lexington, KY 40536
[3]Laboratory of Comparative Pathology, Memorial Sloan-Kettering Cancer Center, New York, NY 10065
[4]Department of Pathology, University of Iowa Carver College of Medicine, Iowa City, IA 52242

IκB kinase β (IKKβ), a central coordinator of inflammatory responses through activation of NF-κB, has been implicated in vascular pathologies, but its role in atherogenesis remains elusive. Here, we demonstrate that IKKβ functions in smooth muscle cells (SMCs) to regulate vascular inflammatory responses and atherosclerosis development. IKKβ deficiency in SMCs driven by a SM22Cre-IKKβ-flox system rendered low density lipoprotein receptor–null mice resistant to vascular inflammation and atherosclerosis induced by high-fat feeding. Unexpectedly, IKKβ–deficient mice were also resistant to diet-induced obesity and metabolic disorders. Cell lineage analysis revealed that SM22Cre is active in primary adipose stromal vascular cells and deficiency of IKKβ diminished the ability of these cells to differentiate, leading to accumulation of adipocyte precursor cells in adipose tissue. Mechanistically, reduction of IKKβ expression or pharmacological inhibition of IKKβ inhibited proteasome-mediated β-catenin ubiquitination and degradation in murine preadipocytes, resulting in elevated β-catenin levels and impaired adipocyte differentiation. Further, chronic treatment of mice with a potent IKKβ inhibitor decreased adipogenesis and ameliorated diet-induced obesity. Our findings demonstrate a pivotal role of IKKβ in linking vascular inflammation to atherosclerosis and adipose tissue development, and provide evidence for using appropriate IKKβ inhibitors in the treatment of obesity and metabolic disorders.

CORRESPONDENCE
Changcheng Zhou:
c.zhou@uky.edu

Abbreviations used: ApoE, apolipoprotein E; BAT, brown adipose tissue; BCA, brachiocephalic artery; COX, cyclooxygenase; EC, endothelial cell; GTT, glucose tolerance test; HF, high fat; IκB, inhibitory of κB protein; IKK, IκB kinase; LDL, low density lipoprotein; MCP-1, monocyte chemotactic protein; MSC, mesenchymal stem cell; PDGFR, platelet-derived growth factor receptor; SMA, smooth muscle actin; SMC, smooth muscle cell; Smurf, Smad ubiquitination regulatory factor; SV, stromal vascular; UCP, uncoupling protein; VCAM, vascular cell adhesion molecule; VLDL, very LDL; WAT, white adipose tissue; WD, Western diet.

Inflammatory responses are the driving force of atherosclerosis development (Libby, 2002; Moore and Tabas, 2011). Many inflammatory pathways that contribute to the development of insulin resistance and atherosclerosis are regulated by the transcription factor NF-κB, a master regulator of the innate and adaptive immune responses (Zhou et al., 2006; Hayden and Ghosh, 2008; Baker et al., 2011). The NF-κB family consists of five members: p65 (RelA), RelB, c-Rel, p100/p52, and p105/p50. NF-κB normally remains in the cytoplasm bound to inhibitor of κB (IκB) proteins. Activating signals, such as proinflammatory cytokines, reactive oxygen species, and viral products lead to activation of IκB kinase (IKK) that phosphorylates IκB and promotes their degradation, allowing NF-κB to translocate to the nucleus and promote transcription of target genes (Hayden and Ghosh, 2008; Park et al.,

2012; Zhou et al., 2006). The IKK complex consists of two kinase subunits, IKKα and IKKβ, and a regulatory subunit NF-κB essential modulator (NEMO, or IKKγ; Karin, 2006; Hayden and Ghosh, 2008). IKKβ is the predominant catalytic subunit of the IKK complex that is required for canonical activation of NF-κB by inflammatory mediators (Karin, 2006; Solinas and Karin, 2010).

IKKβ-mediated NF-κB activation has been implicated in pathogenesis of atherosclerosis (Baker et al., 2011; Moore and Tabas, 2011). Activated NF-κB has been identified in human atherosclerotic plaques and was enhanced in unstable coronary plaques (Brand et al., 1996; Monaco et al., 2004). NF-κB activation in human atherosclerosis was IKKβ-dependent and resulted

J. Xu's present address is Dept. of Medicine, Medical College of Georgia, Augusta, GA.

The Journal of Experimental Medicine

in selective up-regulation of major proinflammatory and pro-thrombotic mediators (Monaco et al., 2004). The negative regulator of NF-κB, A20 affects atherosclerosis development in apolipoprotein E-deficient (ApoE$^{-/-}$) mice (Wolfrum et al., 2007). Atherosclerosis was increased in A20 haploinsufficient and decreased in A20 overexpressing ApoE$^{-/-}$ mice (Wolfrum et al., 2007). Interestingly, bone marrow transplantation of macrophages lacking IKKβ increased atherosclerosis in low density lipoprotein (LDL) receptor-deficient (LDLR$^{-/-}$) mice (Kanters et al., 2003). However, macrophage-specific inhibition of NF-κB by overexpressing trans-dominant, non-degradable forms of IκBα decreased foam-cell formation (Ferreira et al., 2007), and myeloid-specific IκBα deletion promoted atherogenesis in LDLR$^{-/-}$ mice (Goossens et al., 2011). We have recently demonstrated that myeloid-specific IKKβ deficiency decreases diet-induced atherosclerosis in LDLR$^{-/-}$ mice (Park et al., 2012). Although deletion of IKKβ in endo-thelial cells (ECs) resulted in liver degeneration and embryonic lethality (Hou et al., 2008), inhibiting NF-κB activity in ECs by deletion of NEMO or expression of dominant-negative IκBα decreased vascular inflammation and athero-sclerosis in ApoE$^{-/-}$ mice (Gareus et al., 2008). These findings demonstrate that functions of IKKβ–NF-κB in atherosclerosis are complex and further studies are needed to define the cell/tissue-specific role of IKKβ in atherosclerosis.

Smooth muscle cells (SMCs) are a major component of the vascular system and are essential for normal cardiovascular function, yet the role of IKKβ-mediated NF-κB activation by SMCs in atherosclerosis remains elusive. Here, we report that deficiency of IKKβ in SMCs protected LDLR$^{-/-}$ mice from diet-induced vascular inflammation and athero-sclerosis. Unexpectedly, SMC IKKβ-deficient mice were also resistant to diet-induced obesity and associated metabolic disorders. We found that deficiency of IKKβ inhibited the differentiation of adipose stromal vascular (SV) cells or 3T3-L1 preadipocytes into adipocytes. Furthermore, reduction of IKKβ expression or pharmacological inhibition of IKKβ blocked proteasome-mediated β-catenin ubiquitination and degradation in murine preadipocytes, resulting in elevated β-catenin levels and impaired adipocyte differentiation. Lastly, chronic treatment of mice with a potent IKKβ inhibitor decreases adipogenesis and ameliorated diet-induced obesity. These results demonstrate a pivotal role of IKKβ in linking vascular inflammation with adipose development and atherosclerosis.

RESULTS
Generation of LDLR$^{-/-}$ mice with SMC-specific IKKβ deficiency
To investigate the role of IKKβ in SMC function and vascular inflammation, we bred mice carrying loxP-flanked IKKβ alleles (IKKβ$^{F/F}$; Li et al., 2003) with SM22Cre transgenic mice, a widely used model for in vivo analysis of gene function in SMCs (Holtwick et al., 2002), to generate SMC-specific IKKβ knock-out mice (termed SM22Cre$^+$IKKβ$^{F/F}$). To increase susceptibility to atherosclerotic lesion development, SM22Cre$^+$IKKβ$^{F/F}$

mice were crossed with atherosclerosis-prone LDLR$^{-/-}$ mice to generate SM22Cre$^+$IKKβ$^{F/F}$LDLR$^{-/-}$ mice. Western blot analysis confirmed the specific and efficient IKKβ deletion in SMC-abundant aorta but not in other SMC-less abundant tissues of SM22Cre$^+$IKKβ$^{F/F}$LDLR$^{-/-}$ mice (Fig. 1 A). To determine whether deficiency of IKKβ inhibits NF-κB activity in SMCs, vascular SMCs were isolated from aortas of IKKβ$^{F/F}$LDLR$^{-/-}$ and SM22Cre$^+$IKKβ$^{F/F}$LDLR$^{-/-}$ mice and treated with NF-κB stimuli TNF. TNF-induced NF-κB subunit p65 translocation from cytoplasm to nucleus was blocked by deficiency of IKKβ (Fig. 1 B). Electrophoretic mobility shift assay also demonstrated that TNF increased the DNA binding activity of NF-κB in SMCs of IKKβ$^{F/F}$LDLR$^{-/-}$ mice but not in IKKβ-deficient SMCs (Fig. 1 C). To further determine the role of IKKβ in the regulation of SMC inflammation, vascular SMCs were also treated with endotoxin LPS. Gene expression analyses showed that the ability of LPS to induce expression of mRNAs encoding monocyte chemotactic protein-1 (MCP-1), IL-1α, IL-1β, IL-6, and vascular cell adhesion molecule-1 (VCAM-1) was abrogated in SMCs of SM22Cre$^+$IKKβ$^{F/F}$LDLR$^{-/-}$ mice (Fig. 1 D). These results suggest that ablation of IKKβ attenuates NF-κB activity and reduces NF-κB-regulated proinflammatory gene expression in SMCs.

Deficiency of SMC IKKβ inhibits diet-induced vascular inflammation and atherosclerosis development in LDLR$^{-/-}$ mice
To determine the role of SMC IKKβ in atherosclerosis development, 4-wk-old male SM22Cre$^+$IKKβ$^{F/F}$LDLR$^{-/-}$ and IKKβ$^{F/F}$LDLR$^{-/-}$ littermates were fed a standard chow diet or high-fat (HF) Western diet (WD, 21% fat and 0.2% cholesterol) for 12 wk. Whereas no lesions were seen in chow-fed mice (unpublished data), SM22Cre$^+$IKKβ$^{F/F}$LDLR$^{-/-}$ mice developed substantially smaller atherosclerotic lesions in the aorta compared with IKKβ$^{F/F}$LDLR$^{-/-}$ mice when fed a WD (Fig. 2 A). In addition to aorta, deficiency of IKKβ also inhibited atherosclerosis development in the brachiocephalic artery (BCA), an artery prone to developing advanced lesions (Fig. 2 B). Quantification of cross section lesion areas at the aortic root and BCA revealed that SM22Cre$^+$IKKβ$^{F/F}$LDLR$^{-/-}$ mice had 54% decreased lesions at the aortic root (Fig. 2 C) and 48% decreased lesions at the BCA (Fig. 2 D) compared with that of IKKβ$^{F/F}$LDLR$^{-/-}$ mice. Thus, deficiency of IKKβ significantly decreased diet-induced atherosclerosis in LDLR$^{-/-}$ mice.

We next sought to determine whether NF-κB activation in the vasculature is associated with atherosclerosis development. NF-κB–regulated proinflammatory genes were analyzed in aortas of IKKβ$^{F/F}$LDLR$^{-/-}$ and SM22Cre$^+$IKKβ$^{F/F}$LDLR$^{-/-}$ mice. WD feeding significantly increased the expression levels of proinflammatory genes, including MCP-1, IL-1β, cyclooxygenase-2 (COX-2), and VCAM-1, in aortas of IKKβ$^{F/F}$LDLR$^{-/-}$ mice (Fig. 2 E). Further, the expression levels of several key inflammatory cytokines, including IL-1β, TNF, and MCP-1, were decreased in the atherosclerotic lesions and arterial walls
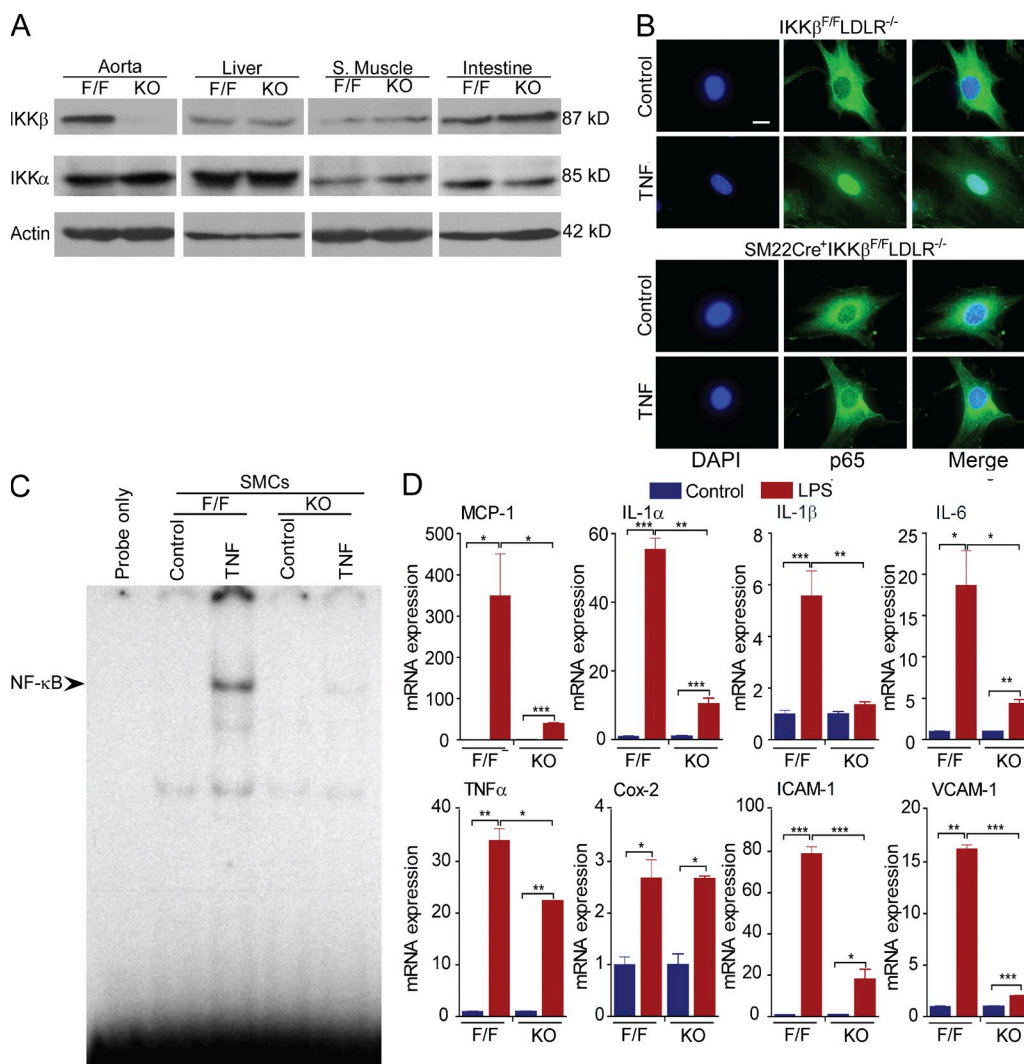
Figure 1. **Generation of LDLR$^{-/-}$ mice with SMC-specific IKKβ deficiency.** (A) Western blot analysis of IKKβ and IKKα expression in aorta, liver, skeletal muscle (s. muscle), and intestine of IKKβ$^{F/F}$LDLR$^{-/-}$ (F/F) and SM22Cre$^+$IKKβ$^{F/F}$LDLR$^{-/-}$ (KO) mice. (B) SMCs isolated from aortas of IKKβ$^{F/F}$LDLR$^{-/-}$ and SM22Cre$^+$IKKβ$^{F/F}$LDLR$^{-/-}$ mice were stimulated with TNF (20 ng/ml) or vehicle for 30 min. Cells stained with anti-p65 primary antibodies, followed by fluorescein-labeled secondary antibodies (green). The nuclei were visualized with DAPI (blue). Bars, 20 μm. (C) SMCs were stimulated with TNF (20 ng/ml) or vehicle for 30 min. Nuclear proteins were extracted and NF-κB binding activity was determined by electrophoretic mobility shift assay. (D) SMCs were treated with LPS (5 μg/ml) or vehicle control for 3 h. Expression of proinflammatory cytokines was analyzed by QPCR (n = 5). Similar results were obtained from at least three independent experiments. All data are means ± SD. *, P < 0.05; **, P < 0.01; ***, P < 0.001.

of SM22Cre$^+$IKKβ$^{F/F}$LDLR$^{-/-}$ mice (Fig. 2 F). Collectively, SM22Cre$^+$IKKβ$^{F/F}$LDLR$^{-/-}$ mice were protected from HF feeding–induced vascular inflammation and atherosclerosis.

IKKβ–deficient mice are resistant to diet–induced obesity

To our surprise, we found that SM22Cre$^+$IKKβ$^{F/F}$LDLR$^{-/-}$ mice were resistant to diet-induced obesity. No significant differences in body weight were observed in chow–fed IKKβ$^{F/F}$ LDLR$^{-/-}$ and SM22Cre$^+$IKKβ$^{F/F}$LDLR$^{-/-}$ mice (Fig. 3 A). Whereas body weight was significantly increased after WD feeding in IKKβ$^{F/F}$LDLR$^{-/-}$ mice, SM22Cre$^+$IKKβ$^{F/F}$LDLR$^{-/-}$ mice resisted WD-induced body weight gain (Fig. 3 A). Lean mass was not affected by IKKβ deficiency or WD feeding (Fig. 3 B), but deficiency of IKKβ significantly reduced

diet–induced fat mass or percent body fat increases (Fig. 3, C and D).

Activation of NF-κB in multiple tissues including liver, adipose tissue, and brain has been implicated in diet-induced obesity and metabolic disorders (Yuan et al., 2001; Arkan et al., 2005; Cai et al., 2005; Zhang et al., 2008; Chiang et al., 2009). We found that the food intake was not affected by IKKβ deficiency (Fig. 3 E), but oxygen consumption was significantly elevated in SM22Cre$^+$IKKβ$^{F/F}$LDLR$^{-/-}$ mice relative to IKKβ$^{F/F}$LDLR$^{-/-}$ littermates (Fig. 3, F and G), which is indicative of increased energy expenditure. However, deficiency of IKKβ did not affect brown adipose tissue (BAT) weight or the expression levels of BAT genes involved in thermogenesis (Fig. 3, H and I). It has been previously reported that HF feeding
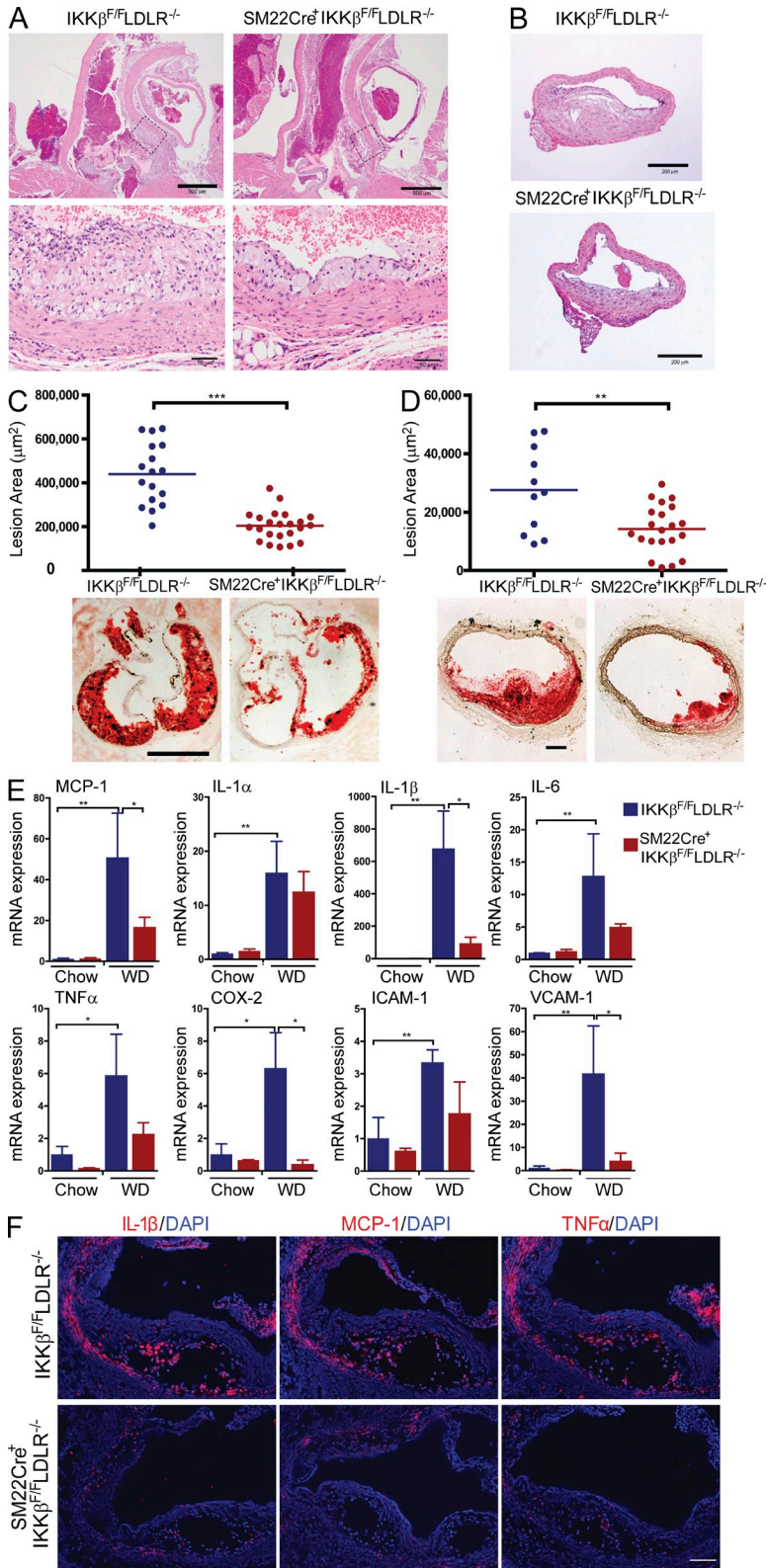
Figure 2. Deficiency of SMC IKKβ inhibits diet–induced vascular inflammation and atherosclerosis development in LDLR⁻/⁻ mice. (A and B) Representative hematoxylin and eosin sections in aorta (A) and BCA (B) of 16-wk-old male IKKβ^F/F^LDLR^−/−^ and SM22Cre⁺IKKβ^F/F^LDLR^−/−^ mice fed a WD for 12 wk. Bottom panels in A represent the magnification of the boxed areas in aorta shown in top panels. (C and D) Quantitative analysis of the lesion area in the aortic root (C) and BCA (D) of WD-fed IKKβ^F/F^LDLR^−/−^ and SM22Cre⁺IKKβ^F/F^LDLR^−/−^ mice ($n = 11$–23 mice). Representative oil red O–stained sections were displayed below the quantification data. (E) Expression of proinflammatory cytokines in aortas of mice fed chow or WD for 12 wk was analyzed by QPCR ($n = 5$ mice). (F) Sections of aortic root atherosclerotic lesions were stained with antibodies against mouse TNF, MCP-1, or IL-1β, followed by fluorescein-labeled secondary antibodies (red). The nuclei were stained with DAPI (blue). A representative figure from three mice per group and the similar result is shown. All data are means ± SD. *, $P < 0.05$; **, $P < 0.01$; ***, $P < 0.001$. Bars: (A, top) 500 µm; (A, bottom) 50 µm; (B) 200 µm; (C) 500 µm; (D) 100 µm; (F) 100 µm.

increases uncoupling protein-1 (UCP-1) expression in white adipose tissue (WAT) and activation of NF-κB decreases UCP-1 expression in WAT, leading to decreased thermogenesis and energy expenditure (Chiang et al., 2009). Indeed, we found that the expression levels of UCP-1 were significantly higher in the WAT of SM22Cre⁺IKKβ^F/F^LDLR^−/−^ mice as compared with
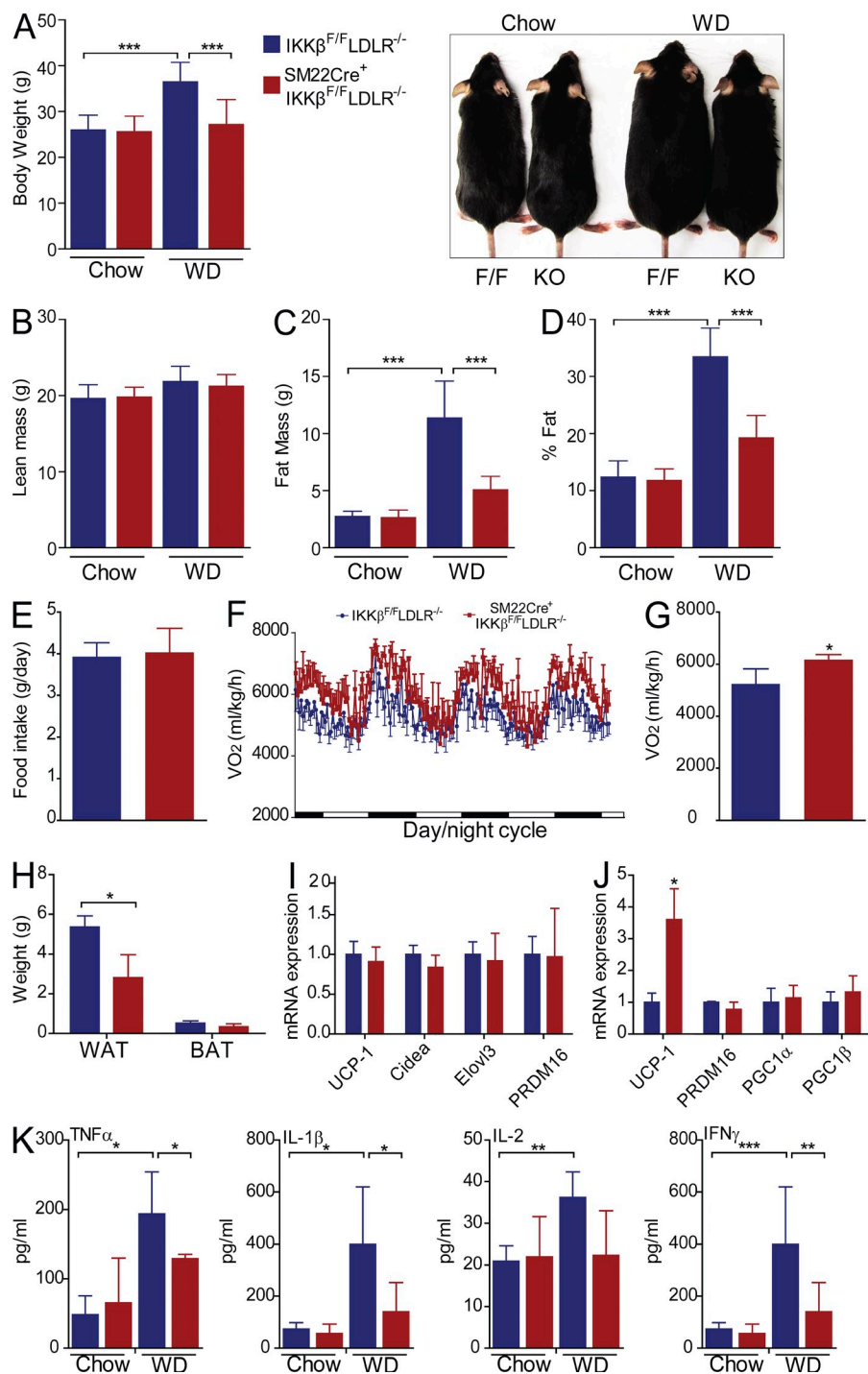
Figure 3. IKKβ–deficient mice are resistant to diet–induced obesity. (A–D) Body weight (A), lean mass (B), fat mass (C), and fat percentage (D) of 16-wk-old male IKKβ$^{F/F}$ LDLR$^{-/-}$ (F/F) and SM22Cre$^+$IKKβ$^{F/F}$LDLR$^{-/-}$ (KO) mice fed a normal chow diet (Chow) or WD for 12 wk (n = 15–20 mice). (E–G) Food intake (E), oxygen consumption (F), and mean oxygen consumption (G) were monitored in WD-fed IKKβ$^{F/F}$LDLR$^{-/-}$ and SM22Cre$^+$IKKβ$^{F/F}$ LDLR$^{-/-}$ mice (n = 5 mice). Oxygen consumption data were normalized by lean body mass and mean from 4-d measurements. (H) WAT (epididymal, subcutaneous, perirenal, and omental WAT) and BAT weight measured in WD-fed IKKβ$^{F/F}$LDLR$^{-/-}$ and SM22Cre$^+$IKKβ$^{F/F}$ LDLR$^{-/-}$ mice (n = 7–8 mice). (I and J) The expression of indicated genes in BAT (I) and WAT (J) was analyzed by QPCR (n = 4–8 mice). (K) Plasma cytokine levels in chow or WD-fed IKKβ$^{F/F}$LDLR$^{-/-}$ and SM22Cre$^+$IKKβ$^{F/F}$LDLR$^{-/-}$ mice (n = 5–7 mice). Results are representative of three independent experiments. All data are means ± SD. *, $P < 0.05$; **, $P < 0.01$; ***, $P < 0.001$.

IKKβ$^{F/F}$LDLR$^{-/-}$ littermates (Fig. 3 J), which may contribute to the increased energy expenditure in IKKβ–deficient mice.

Obesity is associated with chronic inflammation that plays a crucial role in energy imbalance and metabolic disorders (Gregor and Hotamisligil, 2011). We next measured plasma cytokine levels to determine whether SM22Cre$^+$IKKβ$^{F/F}$ LDLR$^{-/-}$ mice had decreased systemic inflammation. WD feeding increased plasma levels of proinflammatory cytokines including TNF, IL-1β, and IFN-γ in IKKβ$^{F/F}$LDLR$^{-/-}$ mice,

and these levels were significantly reduced in SM22Cre$^+$ IKKβ$^{F/F}$LDLR$^{-/-}$ mice (Fig. 3 K). Collectively, deficiency of IKKβ protected mice from diet induced obesity and energy imbalance.

IKKβ–deficient mice are protected against obesity–associated metabolic disorders

Obesity is frequently accompanied by metabolic disorders, including glucose intolerance, hyperlipidemia, and hepatic steatosis.

We next examined whether SM22Cre$^+$IKKβ$^{F/F}$LDLR$^{-/-}$ mice are protected from these disorders. Compared with IKKβ$^{F/F}$ LDLR$^{-/-}$ mice, SM22Cre$^+$IKKβ$^{F/F}$LDLR$^{-/-}$ mice had significantly lower fasting blood glucose and insulin concentrations (Fig. 4 A) and better glucose tolerance after WD feeding (Fig. 4, B and C). Obesity-associated macrophage infiltration contributes to the development of systemic insulin resistance (Olefsky and Glass, 2010). Although it was readily observed in IKKβ$^{F/F}$ LDLR$^{-/-}$ mice, macrophage infiltration was substantially decreased in WAT of SM22Cre$^+$IKKβ$^{F/F}$LDLR$^{-/-}$ mice (Fig. 4 D), indicating that deficiency of SMC IKKβ blocks the increased inflammatory infiltrates in WAT under obese conditions.

Chronic exposure of IKKβ$^{F/F}$LDLR$^{-/-}$ mice to WD also caused liver enlargement, lipid accumulation, and hepatic steatosis, but SM22Cre$^+$IKKβ$^{F/F}$LDLR$^{-/-}$ mice were protected from these detrimental effects (Fig. 4, E and F). Consistently, hepatic triglyceride and cholesterol contents were significantly reduced in SM22Cre$^+$IKKβ$^{F/F}$LDLR$^{-/-}$ mice (Fig. 4 G).

We also found that WD-induced severe hyperlipidemia was ameliorated in SM22Cre$^+$IKKβ$^{F/F}$LDLR$^{-/-}$ (Fig. 4 H). Fast-performance liquid chromatography (FPLC) analysis of cholesterol distribution patterns showed that SM22Cre$^+$IKKβ$^{F/F}$ LDLR$^{-/-}$ mice had reduced plasma VLDL and LDL cholesterol levels (Fig. 4 I). We next examined the mRNA levels of hepatic lipogenic genes and found that the expression levels of several key lipogenic genes, including SREBP1c, SCD-1, and PPARγ were significantly decreased in the liver of SM22Cre$^+$ IKKβ$^{F/F}$LDLR$^{-/-}$ mice (Fig. 4 J). Collectively, these results suggest that deficiency of IKKβ protected mice from diet-induced obesity and associated metabolic disorders.

Deficiency of IKKβ decreases atherosclerosis in LDLR$^{-/-}$ mice in the absence of HF diet–induced obesity and severe hyperlipidemia

Because WD-fed SM22Cre$^+$IKKβ$^{F/F}$LDLR$^{-/-}$ mice had ameliorated obesity and hyperlipidemia compared with
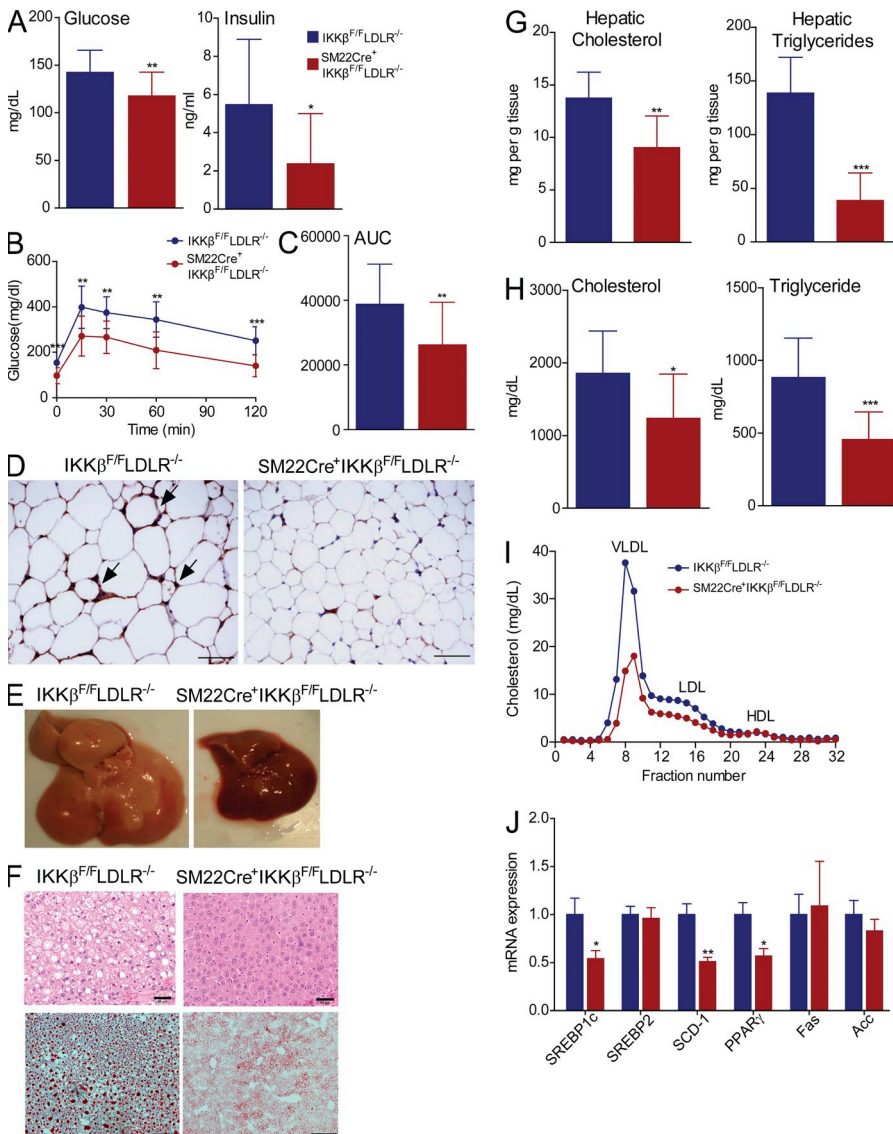

Figure 4. **Deficiency of IKKβ protects mice from obesity-associated metabolic disorders.** (A–C) Fasting plasma glucose and insulin levels (n = 10–15 mice; A), GTT (B), and the area under the curve (AUC) of GTT (C) in 16-wk-old male IKKβ$^{F/F}$LDLR$^{-/-}$ and SM22Cre$^+$IKKβ$^{F/F}$LDLR$^{-/-}$ mice fed a WD for 12 wk (n = 10–15 mice). (D) Macrophage infiltration in WAT determined by F4/80 staining. (E and F) Representative appearance (E) and hematoxylin and eosin (top) and oil red O–stained (bottom) sections (F) of livers. (G–I) Hepatic cholesterol and triglyceride levels (G), plasma cholesterol and triglyceride levels (H), and plasma cholesterol distribution (I) of WD-fed IKKβ$^{F/F}$LDLR$^{-/-}$ and SM22Cre$^+$IKKβ$^{F/F}$LDLR$^{-/-}$ mice (n = 6–10 mice). (J) Hepatic gene expression was analyzed by QPCR (n = 4–8 mice). Results are representative of three independent experiments. All data are means ± SD. *, P < 0.05; **, P < 0.01; ***, P < 0.001. Bars: (D) 100 μm; (F) 50 μm (top) and 200 μm (bottom).
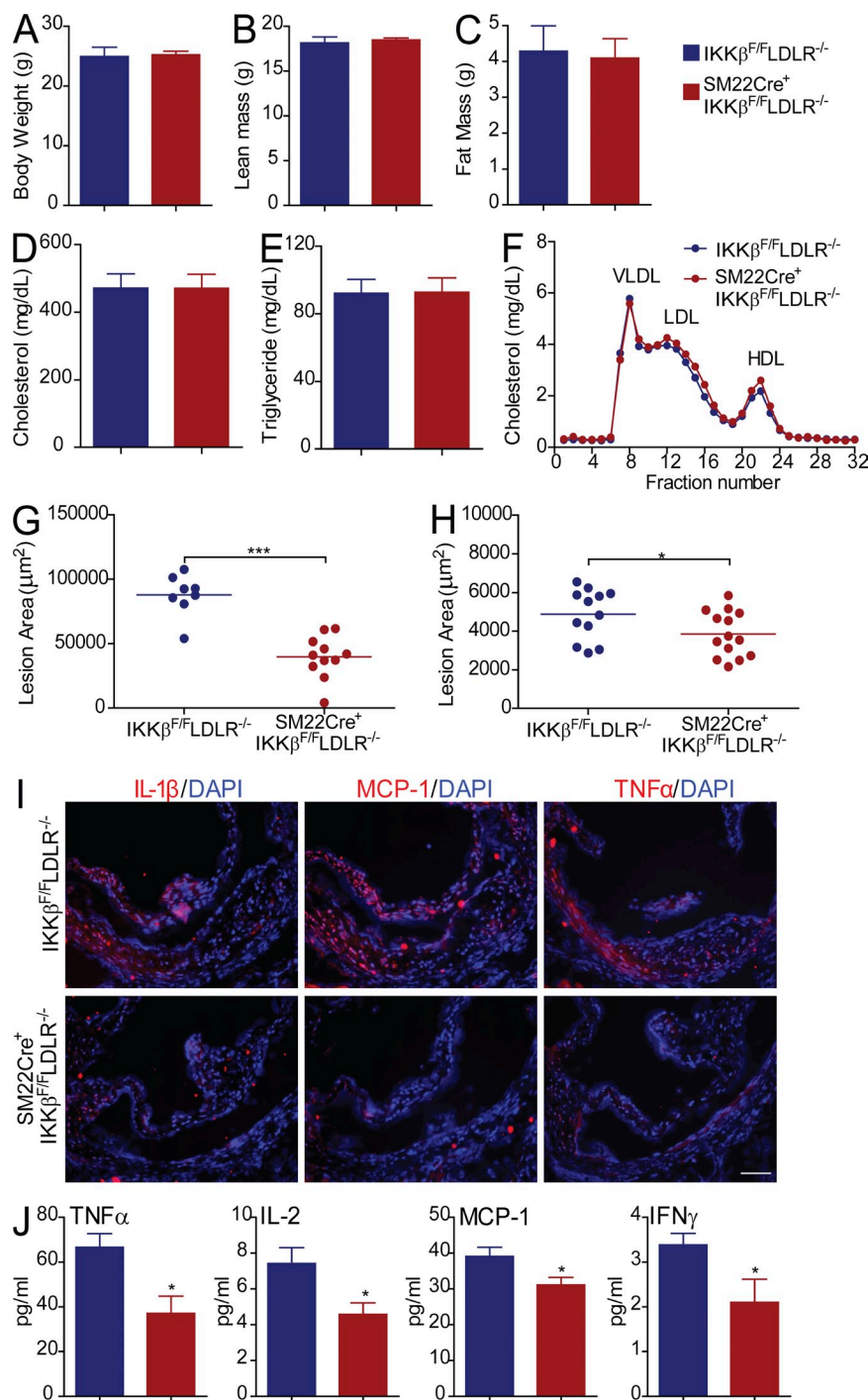
Figure 5. Deficiency of IKKβ reduces atherosclerosis in LDLR$^{-/-}$ mice in the absence of obesity and severe hyperlipidemia. (A–F) Body weight (A), lean mass (B), fat mass (C), plasma cholesterol levels (D), triglyceride (E), and cholesterol distribution (F) of 16-wk-old male IKKβ$^{F/F}$LDLR$^{-/-}$ and SM22Cre$^+$IKKβ$^{F/F}$LDLR$^{-/-}$ mice fed a low-fat AIN76 diet for 12 wk (n = 6–10 mice). (G and H) Quantitative analysis of the lesion area in the aortic root (G) and BCA (H). n = 8–14 mice. (I) Sections of aortic root atherosclerotic lesions were stained with antibodies against mouse TNF, MCP-1, or IL-1β, followed by fluorescein-labeled secondary antibodies (red). The nuclei were stained with DAPI (blue). A representative figure from three mice per group and the similar result is shown. (J) Plasma cytokine levels of AIN76 diet-fed mice (n = 6 mice). Results are representative of three independent experiments. All data are mean ± SD. *, $P < 0.05$; ***, $P < 0.001$. Bars, 100 μm.

IKKβ$^{F/F}$LDLR$^{-/-}$ mice, it is possible that decreased atherosclerosis in these mice was only the secondary effect of improved obesity or plasma lipid levels. To address this issue, we fed SM22Cre$^+$IKKβ$^{F/F}$LDLR$^{-/-}$ and IKKβ$^{F/F}$LDLR$^{-/-}$ littermates a modified semisynthetic low-fat (4.3%) and low–cholesterol (0.02%) AIN76 diet to avoid the additional stresses of obesity and insulin resistance presented in WD-fed model (Teupser et al., 2003). The modified AIN76 diet has been successfully used to induce inflammation and atherosclerosis in LDLR$^{-/-}$ or ApoE$^{-/-}$ mice without causing additional obesity and associated metabolic

disorders in many studies (Teupser et al., 2003; Wolfrum et al., 2007; Sui et al., 2011; Zhou et al., 2011). Indeed, AIN76 diet-fed SM22Cre$^+$IKKβ$^{F/F}$LDLR$^{-/-}$ mice had similar body weight, body composition, and plasma lipid levels compared with IKKβ$^{F/F}$LDLR$^{-/-}$ littermates (Fig. 5, A–F). Nevertheless, SM22Cre$^+$IKKβ$^{F/F}$LDLR$^{-/-}$ mice still had significantly decreased atherosclerotic lesion sizes in the aortic root and BCA compare with control littermates (Fig. 5, G and H). Immunofluorescence staining showed that the expression of MCP-1, TNF, and IL-1β was also decreased in the atherosclerotic lesions
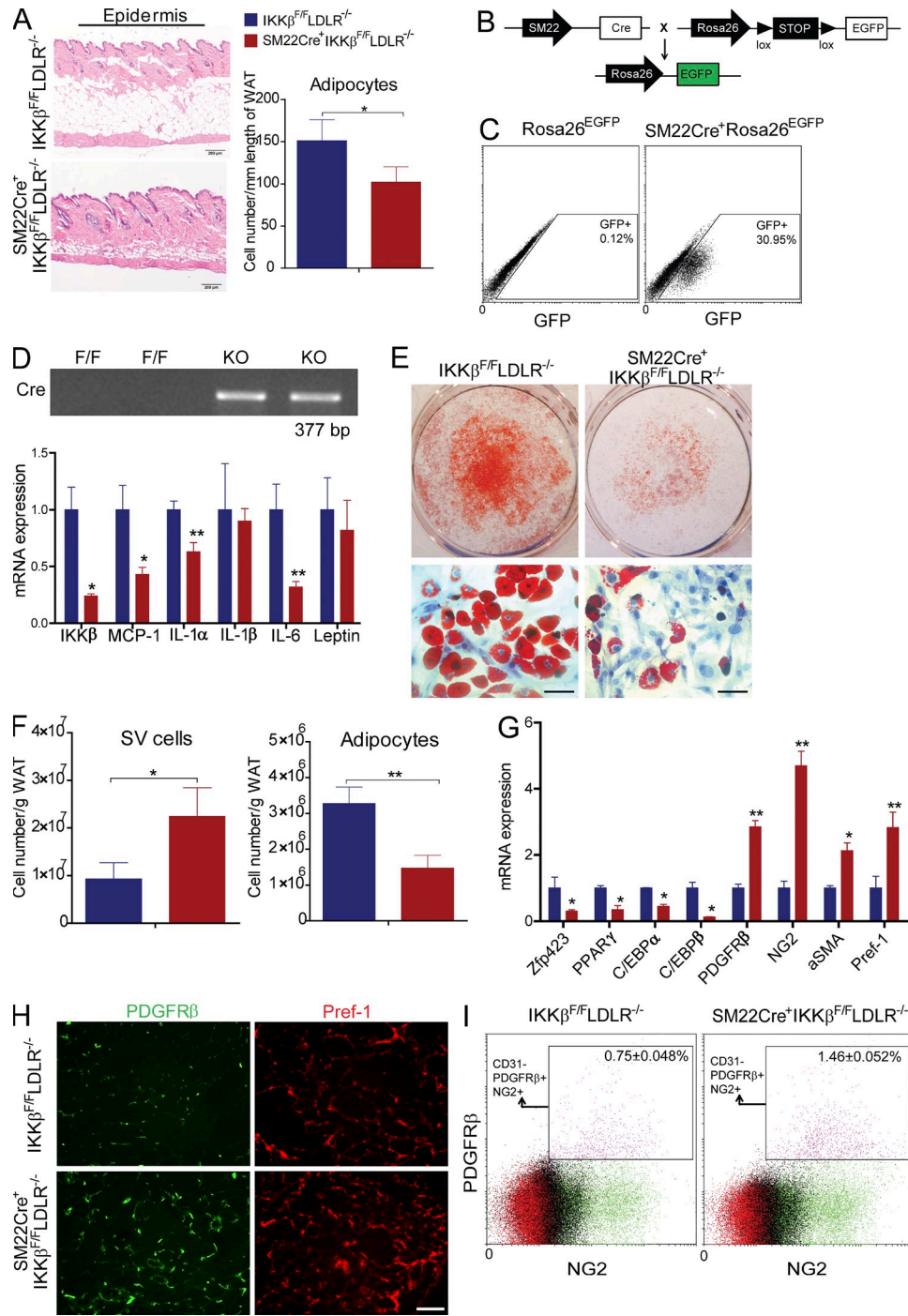
Figure 6. SM22Cre–mediated IKKβ ablation blocks white adipose differentiation. (A) Hematoxylin and eosin staining of transverse sections of subcutaneous WAT from WD-fed IKKβ$^{F/F}$LDLR$^{-/-}$ and SM22Cre$^+$IKKβ$^{F/F}$LDLR$^{-/-}$ mice. The adipocyte numbers were calculated based on per mm epidermal length (n = 5 mice). (B) Schematic of the SM22Cre$^+$Rosa26^{EGFP} mouse model. (C) Quantitation of GFP$^+$ cells in cultures of adipose SV cells isolated from Rosa26^{EGFP} and SM22Cre$^+$Rosa26^{EGFP} mice by flow cytometry. The percentage of GFP$^+$ cells are as indicated in the flow profiles. (D) PCR analysis of genomic DNA from adipose SV cells of IKKβ$^{F/F}$LDLR$^{-/-}$ (F/F) and SM22Cre$^+$IKKβ$^{F/F}$LDLR$^{-/-}$ (KO) mice (top). Expression levels of IKKβ, inflammatory genes, and leptin in adipose SV cells were analyzed by QPCR (n = 3 mice) (bottom). (E) Oil red O staining of adipose SV cells of IKKβ$^{F/F}$LDLR$^{-/-}$ and SM22Cre$^+$IKKβ$^{F/F}$LDLR$^{-/-}$ mice induced by differentiation medium. The nuclei were stained with hematoxylin (blue) in the bottom panel. (F) SV cells and mature adipocytes were isolated from WAT of WD-fed IKKβ$^{F/F}$LDLR$^{-/-}$ and SM22Cre$^+$IKKβ$^{F/F}$LDLR$^{-/-}$ mice. The cell population was displayed as cell number per gram of WAT (n = 5 mice). (G) Expression of adipogenic genes and adipocyte precursor cell markers in adipose SV cells was measured by QPCR (n = 5–7 mice). (H) Sections of subcutaneous WAT were stained with antibodies against adipocyte progenitor markers PDGFRβ and preadipocyte marker Pref-1, followed by Alexa Fluor 488 (green)– or Alexa Fluor 594 (red)–labeled secondary antibodies. A representative figure from three mice per group and

of SM22Cre$^+$IKKβ$^{F/F}$LDLR$^{-/-}$ mice (Fig. 5 I). In addition, the plasma levels of proinflammatory cytokines such as TNF and MCP-1 were also reduced in SM22Cre$^+$IKKβ$^{F/F}$LDLR$^{-/-}$ mice (Fig. 5 J). These results confirm that deficiency of SMC IKKβ inhibits atherosclerotic lesional formation and reduces inflammation in the absence of HF diet–induced obesity or severe hyperlipidemia.

SM22Cre is active in adipose SV cells and causes reduced IKKβ expression in SV cells

It is intriguing that deficiency of IKKβ inhibits HF feeding–induced obesity. Adipocyte number can be a major determinant of fat mass in adults (Rodeheffer et al., 2008; Spalding et al., 2008). Interestingly, we found that WD-fed SM22Cre$^+$IKKβ$^{F/F}$LDLR$^{-/-}$ mice had significantly decreased adipocyte numbers in WAT (Fig. 6 A), indicating that deficiency of IKKβ might affect adipocyte differentiation. A subset of mural cells (SMCs and SMC–like pericytes) that reside in the adipose vasculature have been identified as adipocyte progenitors (Rodeheffer et al., 2008; Tang et al., 2008). Adipocyte progenitors can be isolated from the SV fraction of adipose tissue, a heterogeneous mixture of cells defined by enzymatic dissociation of adipose depots by density separation (Tang et al., 2008; Zeve et al., 2009). To determine whether SM22Cre is active in adipose SV cells, SM22Cre mice were crossed with Rosa26^{EGFP} reporter mice (Mao et al., 2001) that express enhanced GFP (EGFP) in target tissues upon Cre-mediated excision of a "Stop" sequence to generate SM22Cre$^+$Rosa26^{EGFP} mice (Fig. 6 B). SV cells were plated in culture to eliminate nonadherent blood cells, and then allowed to proliferate for 4 d to enrich fibroblastic cells (Gupta et al., 2012). We then used flow cytometry to analyze GFP$^+$ SV cells isolated from WAT of SM22Cre$^+$Rosa26^{EGFP} and Rosa26^{EGFP} littermates. Whereas almost no GFP$^+$ SV cells from Rosa26^{EGFP} control mice were detected by flow cytometry, >30% of cells in the SV culture of SM22Cre$^+$Rosa26^{EGFP} mice were GFP$^+$ cells (Fig. 6 C).

Consistent with cell lineage results, PCR analysis showed that Cre is present in SV cells of SM22Cre$^+$IKKβ$^{F/F}$LDLR$^{-/-}$ but not in IKKβ$^{F/F}$LDLR$^{-/-}$ mice (Fig. 6 D). Accordingly, the mRNA levels of IKKβ and NF-κB–mediated inflammatory genes, including MCP-1, IL-1α, and IL-6, were significantly reduced in SV cells of SM22Cre$^+$IKKβ$^{F/F}$LDLR$^{-/-}$ mice (Fig. 6 D). However, the leptin levels were not affected by IKKβ deficiency in SV cells, which might be due to the low expression levels of leptin in preadipocytes (Melzner et al., 2002). These results suggest that SM22Cre is active in adipose SV cells, resulting in decreased IKKβ and NF-κB target gene expression in these cells.

Ablation of IKKβ inhibits adipocyte differentiation and promotes accumulation of adipocyte precursor cells in WAT

We next tested the adipogenic potential of SV cells from IKKβ$^{F/F}$LDLR$^{-/-}$ and SM22Cre$^+$IKKβ$^{F/F}$LDLR$^{-/-}$ mice to determine the effects of deficiency of IKKβ on adipocyte differentiation. Adipose SV cells of SM22Cre$^+$IKKβ$^{F/F}$LDLR$^{-/-}$ mice differentiated poorly compared with that of IKKβ$^{F/F}$LDLR$^{-/-}$ mice (Fig. 6 E). Consistently, WAT of WD-fed SM22Cre$^+$IKKβ$^{F/F}$LDLR$^{-/-}$ mice had significantly increased SV cell numbers and decreased mature adipocyte numbers as compared with IKKβ$^{F/F}$LDLR$^{-/-}$ mice (Fig. 6 F). The expression levels of key regulators of adipogenesis, including PPARγ, C/EBPα, C/EBPβ, and Zfp423 were significantly decreased in SV cells of SM22Cre$^+$IKKβ$^{F/F}$LDLR$^{-/-}$ mice (Fig. 6 G). In contrast, the expression levels of adipocyte progenitor markers including platelet-derived growth factor receptor β (PDGFRβ), NG2, and α smooth muscle actin (αSMA; Tang et al., 2011; Tang et al., 2008), as well as the preadipocyte marker, Pref-1, were significantly increased in the SV cells of SM22Cre$^+$IKKβ$^{F/F}$LDLR$^{-/-}$ mice (Fig. 6 G), indicating accumulation of adipocyte precursor cells in WAT. Indeed, immunofluorescence staining showed that SM22Cre$^+$IKKβ$^{F/F}$LDLR$^{-/-}$ mice held abundant PDGFRβ$^+$ or Pref-1$^+$ cells in WAT compared with IKKβ$^{F/F}$LDLR$^{-/-}$ mice (Fig. 6 H). SV cells were further analyzed for PDGFRβ, NG2, and EC marker CD31 expression by flow cytometry (Fig. S1). Consistent with gene expression and immunostaining results, deficiency of IKKβ significantly increased the CD31$^-$PDGFRβ$^+$NG2$^+$ SV cell population in WAT of SM22Cre$^+$IKKβ$^{F/F}$LDLR$^{-/-}$ mice (Fig. 6 I). Collectively, these results suggest that ablation of IKKβ inhibits adipocyte differentiation and white adipose development, leading to accumulation of adipocyte precursor cells in WAT.

Deficiency of IKKβ inhibits β–catenin ubiquitination and degradation in murine preadipocytes

To further characterize the novel role of IKKβ in adipogenesis, we investigated whether IKKβ can also regulate the differentiation of 3T3-L1 cells, a well-established cell culture system to study adipocyte differentiation (Cawthorn et al., 2012; Tang and Lane, 2012). Interestingly, 3T3-L1 cells also expressed multiple SMC or mural cell markers, including SM22, αSMA, and PDGFRβ (Fig. 7 A). Whereas differentiation medium rapidly increased the expression levels of adipocyte markers including aP2 and adiponectin in 3T3-L1 cells, the expression levels of the preadipocyte marker Pref-1 and mural cell markers were reduced or diminished after 48 h (Fig. 7 A), indicating a fast cell fate transition. Next, we used lentiviral vectors harboring short hairpin RNAs (shRNAs) directed

the similar result is shown. (I) Adipose SV cells were examined for expression of adipocyte progenitor cell makers, PDGFRβ, and NG2, and endothelial cell marker CD31 with flow cytometry. CD31$^+$, NG2$^+$, and CD31$^-$NG2$^-$ cells are highlighted with red, green, and black, respectively. The percentages of CD31$^-$PDGFRβ$^+$NG2$^+$ cells are as indicated in the flow profiles (P < 0.001, *n* = 3–4 mice). Similar results were obtained from at least three independent experiments. All data are means ± SD. *, P < 0.05; **, P < 0.01. Bars: (A) 200 μm; (E, bottom) 50 μm; (H) 100 μm.

against IKKβ to establish stable IKKβ–deficient 3T3-L1 clones (Fig. 7 B). Consistent with SV cell results (Fig. 6 E), reduction of IKKβ expression also inhibited 3T3-L1 cell differentiation (Fig. 7 C).

To understand the molecular mechanism by which IKKβ–NF-κB regulates adipocyte differentiation, we tested several key signaling pathways associated with adipocyte differentiation. Interestingly, we found that shRNA–mediated IKKβ
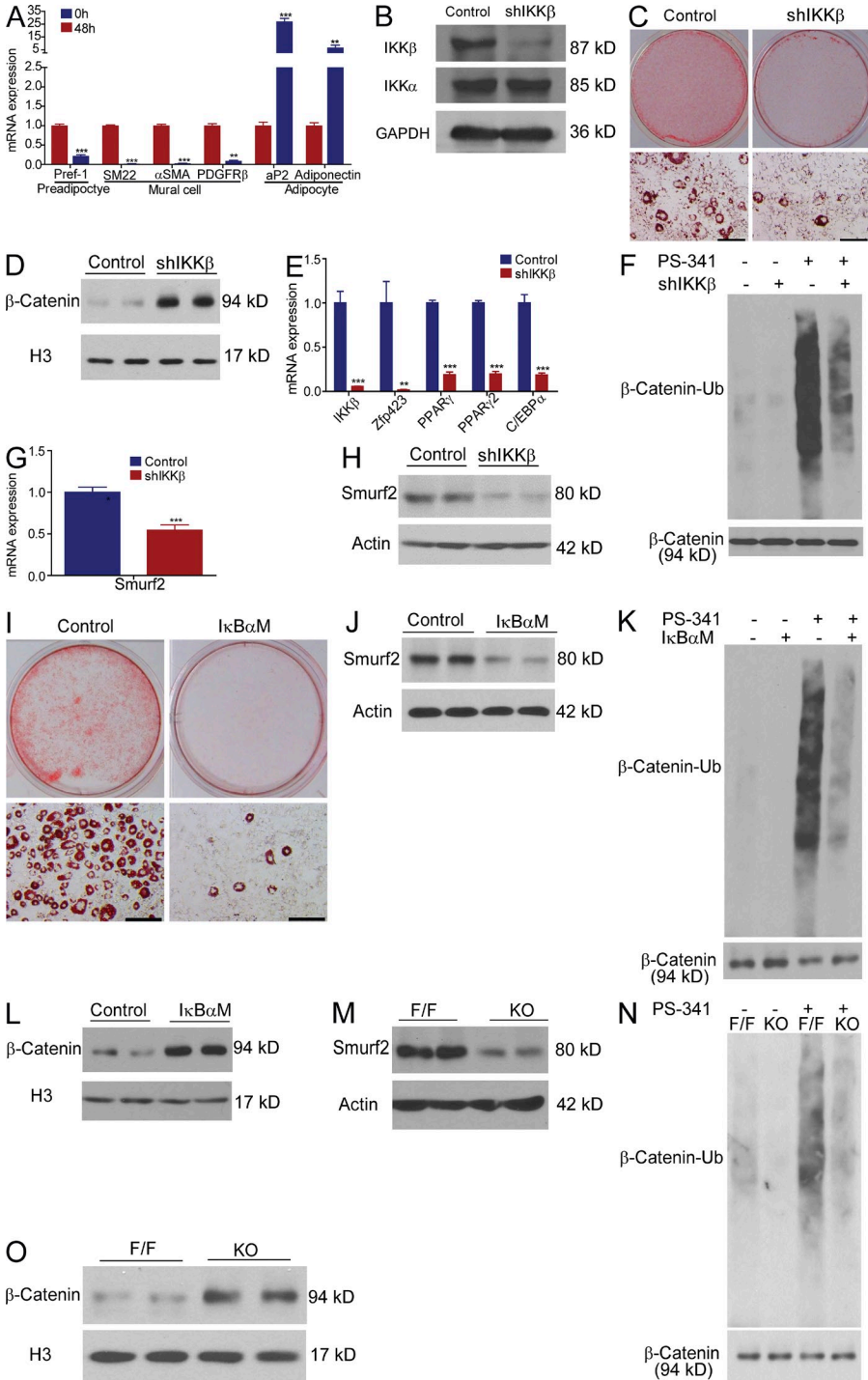

Figure 7. IKKβ regulates β–catenin ubiquitination and adipocyte differentiation. (A) Expression levels of preadipocyte, mural cell, and mature adipocyte markers in 3T3-L1 cells at 0 and 48 h after addition of differentiation media (*n* = 3). (B) Western blot analysis of IKKβ and IKKα levels in 3T3-L1 preadipocytes expressing control shRNA or shRNA against IKKβ (shIKKβ). (C) Oil red O staining of control or shIKKβ 3T3-L1 cells induced by differentiation medium. (D) Western blot analysis of nuclear β-catenin protein levels of control or shIKKβ 3T3-L1 cells. Nuclear proteins were also probed with anti-Histone H3 antibodies as an internal control. (E) QPCR analysis of expression of IKKβ and adipogenic genes in control or shIKKβ 3T3-L1 cells (*n* = 3–5). (F) Control or shIKKβ 3T3-L1 cells were treated with vehicle control or 100 nM PS-341 as indicated for 4 h. β-catenin was immunoprecipitated with anti–β-catenin antibodies, and then probed with antiubiquitin monoclonal antibodies. The whole cell lysates were probed with anti–β-catenin antibodies as an internal control. (G) QPCR analysis of Smurf2 expression in control or shIKKβ 3T3-L1 cells (*n* = 4). (H) Western blot analysis of Smurf2 protein levels in control or shIKKβ 3T3-L1 cells. (I) Oil red O staining of 3T3-L1 cells transfected with control vector or vector expressing IκBαM induced by differentiation medium. (J) Western blot analysis of Smurf2 protein levels in 3T3-L1 cells expressing control or IκBαM vectors. (K) Control or IκBαM-expressing 3T3-L1 cells were treated with vehicle control or 100 nM PS-341 as indicated for 4 h. β-catenin was immunoprecipitated with anti–β-catenin antibodies and then probed with anti-ubiquitin monoclonal antibodies. The whole-cell lysates were probed with anti–β-catenin antibodies as an internal control. (L) Western blot analysis of nuclear β-catenin levels in control or IκBαM-expressing 3T3-L1 cells. Nuclear proteins were probed with anti-Histone H3 antibodies as an internal control. (M) Western blot analysis of Smurf2 levels in adipose SV cells isolated from WD-fed IKKβ[F/F]LDLR^{−/−} (F/F) and SM22Cre[+]IKKβ[F/F]LDLR^{−/−} (KO) mice. (N) Adipose SV cells were treated with vehicle control or 100 nM PS-341, as indicated, for 4 h. β-catenin was immunoprecipitated with anti–β-catenin antibodies and then probed with anti-ubiquitin monoclonal antibodies. The whole cell lysates were probed with anti–β-catenin antibodies as an internal control. (O) Western blot analysis of nuclear β-catenin levels in SV cells. Nuclear proteins were probed with anti-Histone H3 antibodies as internal control. Similar results were obtained from at least three independent experiments. All data are means ± SD. **, P < 0.01; ***, P < 0.001. Bar: (C, bottom) 100 µm; (I, bottom) 100 µm.

knockdown increased nuclear β-catenin protein levels in 3T3-L1 cells (Fig. 7 D). Wnt–β-catenin signaling has been well defined to inhibit adipogenesis in vitro and in vivo (Ross et al., 2000; Wright et al., 2007; Cristancho and Lazar, 2011). Consistent with decreased adipogenesis, several key adipogenic genes were repressed in shIKKβ 3T3-L1 cells (Fig. 7 E). Because β-catenin degradation is regulated by ubiquitin–proteasome pathway, we then used a well-characterized proteasome inhibitor, PS-341 (Hideshima et al., 2001; Chang et al., 2013), to determine whether IKKβ–NF-κB signaling can modulate β-catenin ubiquitination in 3T3-L1 preadipocytes. Knockdown of IKKβ substantially inhibited β-catenin ubiquitination as detected by antiubiquitin antibodies (Fig. 7 F). We also found that the mRNA levels of Smad ubiquitination regulatory factor 2 (Smurf 2), a known NF-κB target gene (Chang et al., 2013), were significantly decreased in IKKβ-knockdown 3T3-L1 cells (Fig. 7 G). Western blot analysis further confirmed the decreased protein levels of Smurf2 in shIKKβ 3T3-L1 cells (Fig. 7 H). Smurf2 is an ubiquitin E3 ligase responsible for proteasome-mediated degradation of several proteins including β-catenin (Han et al., 2006; Millar, 2006; Chang et al., 2013). Therefore, the decreased Smurf2 levels likely leads to inhibited β-catenin ubiquitination and degradation.

To determine whether IKKβ regulates 3T3-L1 cell differentiation through the canonical NF-κB pathway, we overexpressed a nondegradable form of NF-κB inhibitor, IκBαM, which contains serine to alanine mutations in amino acids 32 and 36 (Zhou et al., 2006) in 3T3-L1 cells. Expression of IκBαM also inhibited 3T3-L1 cell differentiating into adipocytes (Fig. 7 I). Consistently, the expression levels of Smurf2 were suppressed in IκBαM-overexpressed 3T3L1 cells (Fig. 7 J). Overexpression of IκBαM also blocked β-catenin ubiquitination and degradation (Fig. 7 K), resulting in β-catenin accumulation in nuclei of 3T3-L1 cells (Fig. 7 L). Next, we tested whether IKKβ regulates β-catenin ubiquitination in primary adipose SV cells. The protein levels of Smurf2 were decreased in SV cells of SM22Cre$^+$IKKβ$^{F/F}$LDLR$^{-/-}$ mice (Fig. 7 M). As expected, deficiency of IKKβ decreased β-catenin ubiquitination (Fig. 7 N) and increased nuclear β-catenin levels (Fig. 7 O) in SV cells of SM22Cre$^+$IKKβ$^{F/F}$LDLR$^{-/-}$ as compared with that of IKKβ$^{F/F}$LDLR$^{-/-}$ mice. Collectively, these results indicate that deficiency of IKKβ inhibited proteasome-mediated β-catenin ubiquitination and degradation in murine preadipocytes, leading to elevated β-catenin levels and impaired adipocyte differentiation.

Pharmacological inhibition of IKKβ decreases adipogenesis and ameliorates diet–induced obesity in mice

IKKβ inhibitors such as salicylates have long been used to treat inflammatory conditions including diabetes in humans (Williamson, 1901; Reid et al., 1957; Kim et al., 2001; Yuan et al., 2001). We next used a highly selective IKKβ inhibitor, BMS–345541 (Burke et al., 2003; Lancaster et al., 2012), to determine whether pharmacological inhibition of IKKβ can affect 3T3-L1 cell differentiation. Indeed, BMS–345541 inhibited 3T3-L1 differentiation in a dose–dependent manner

(Fig. 8 A). BMS–345541 did not affect IKKβ expression levels but significantly reduced the expression levels of Smurf2 and several key adipogenic genes (Fig. 8 B). Further, BMS–345541 also inhibited β-catenin ubiquitination (Fig. 8 C) and promoted β-catenin accumulation (Fig. 8 D) in nuclei of 3T3-L1 cells. In addition to BMS–345541, the relatively weak IKKβ inhibitor sodium salicylate also inhibited 3T3-L1 cell differentiation at relatively high doses (Fig. 8 E), indicating that salicylates may also have beneficial effects on obesity when used at high concentrations.

We next determined whether chronic inhibition of IKKβ activity can ameliorate diet–induced obesity. Groups of 8–wk-old wild–type male C57BL/6 mice were fed a WD and treated with vehicle control or 10 mg/kg body weight BMS–345541 by daily oral gavage for 8 wk (Fig. 9 A). Interestingly, BMS–345541 treatment significantly decreased diet–induced body weight gain and adiposity (Fig. 9, A–C). Whereas the lean mass was not affected, BMS–345541 treatment significantly decreased the fat mass (Fig. 9 B). Both epididymal and subcutaneous fat pads were markedly smaller in mice treated with BMS–345541 (Fig. 9 C). Further, the expression levels of NF-κB target genes including Smurf2 were significantly decreased in WAT of BMS–345541-treated mice (Fig. 9 D). Consistently, BMS–345541 treatment also elevated the nuclear β-catenin levels in WAT (Fig. 9 E). Next, adipose SV cells were isolated from control or BMS–345541–treated mice for differentiation assays. Consistent with in vitro results (Fig. 8), the adipogenic potential of SV cells from BMS–345541–treated mice were markedly impaired (Fig. 9 F). β-Catenin ubiquitination in SV cells of BMS-treated mice was also inhibited as detected by antiubiquitin antibodies (Fig. 9 G). Collectively, these results indicate that pharmacological inhibition of IKKβ can decrease adipogenesis and ameliorate diet–induced obesity.

DISCUSSION

The role of IKKβ–NF-κB pathway in the regulation of inflammatory responses has been extensively studied, but the role of this pathway in the development of inflammation–associated metabolic disorders and atherosclerosis remains elusive. Previous studies have mainly focused on the function of IKKβ–NF-κB in inflammatory cells (e.g., monocytes and macrophages) involved in atherogenesis (Kanters et al., 2003; Ferreira et al., 2007; Goossens et al., 2011; Park et al., 2012). In the present study, we found that HF feeding induced a localized and strong inflammatory response in the vasculature. SM22Cre-mediated deletion of IKKβ reduced NF-κB-regulated proinflammatory gene expression in SMCs and SM22Cre$^+$IKKβ$^{F/F}$LDLR$^{-/-}$ mice had attenuated vascular inflammation and decreased atherosclerosis elicited by HF feeding. We also used a low-fat AIN76 diet to determine whether deficiency of SMC IKKβ affected atherosclerosis development without WD-induced obesity and metabolic disorders. As expected, the lesion sizes were smaller in AIN76 diet-fed LDLR$^{-/-}$ mice compared with the WD-fed mice. Nevertheless, deficiency of IKKβ still significantly decreased the
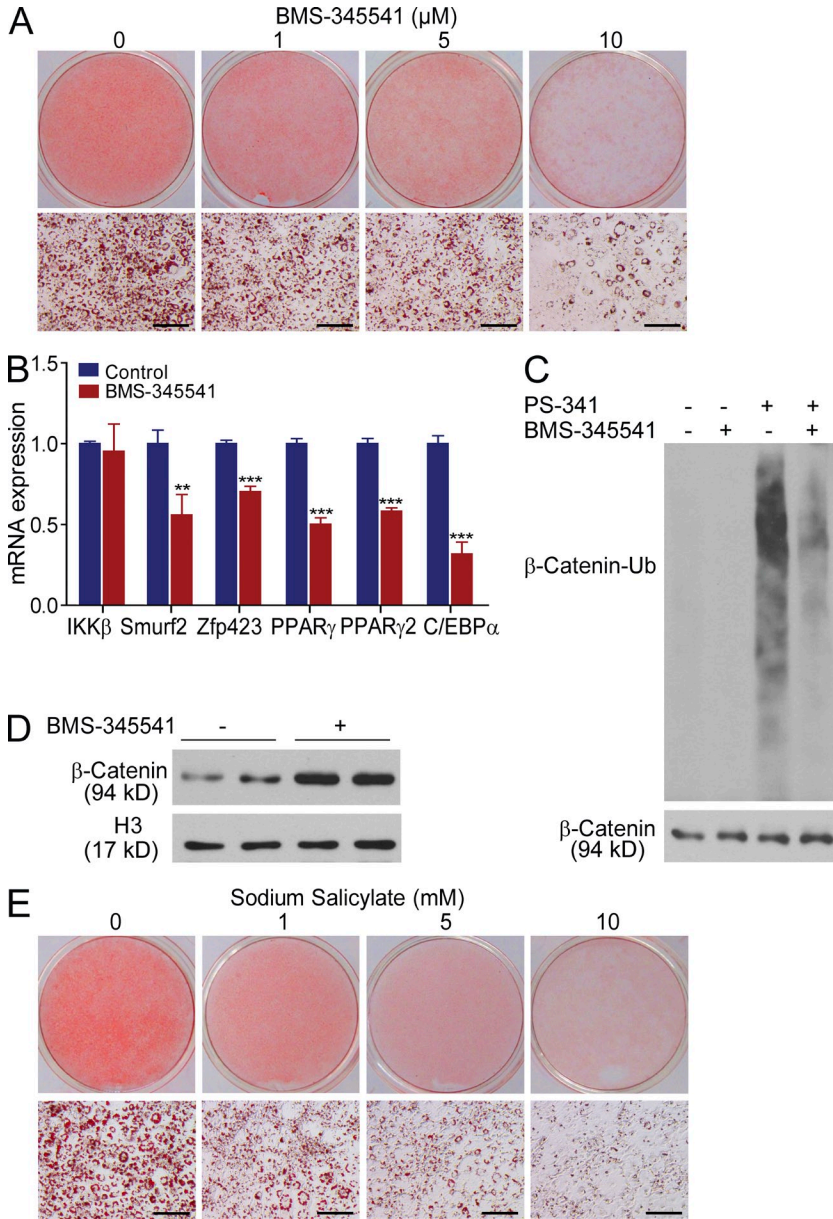
Figure 8. Pharmacological inhibition of IKKβ inhibits adipocyte differentiation. (A) Oil red O staining of 3T3-L1 cells induced by differentiation medium or medium containing IKKβ inhibitor BMS-345541 at indicated concentrations. (B) Analysis of IKKβ, Smurf2, and adipogenic genes in 3T3-L1 cells treated with control or 10 μM BMS-345541 for 48 h by QPCR ($n = 3$–5). (C) 3T3-L1 cells were treated with vehicle control or 10 μM BMS-345541 for 48 h before incubating with vehicle control or 100 nM PS-341 for 4 h. β-catenin was immunoprecipitated with anti–β-catenin antibodies, and then probed with antiubiquitin monoclonal antibodies. The whole-cell lysates were probed with anti–β-catenin antibodies as an internal control. (D) Western blot analysis of nuclear β-catenin levels in 3T3-L1 cells treated with vehicle control or 10 μM BMS-345541 for 48 h. Nuclear proteins were probed with anti-Histone H3 antibodies as an internal control. (E) Oil red O staining of 3T3-L1 cells induced by differentiation medium or medium containing IKKβ inhibitor sodium salicylate at indicated concentrations. Similar results were obtained from at least three independent experiments. All data are mean ± SD. **, $P < 0.01$; ***, $P < 0.001$. Bars: (A, bottom) 100 μm; (E, bottom) 100 μm.

atherosclerotic lesions and reduced lesional inflammation in the absence of HF feeding-elicited obesity and severe hyperlipidemia. Therefore, deficiency of SMC IKKβ not only decreased the WD-induced large lesions but also reduced the AIN76 diet-induced moderate lesions. Although the precise role of inflammatory cell IKKβ–NF-κB in atherogenesis still needs further characterization (Kanters et al., 2003; Ferreira et al., 2007; Goossens et al., 2011; Park et al., 2012), inhibition of NF-κB activity in ECs decreased vascular inflammation and atherosclerosis in ApoE$^{-/-}$ mice (Gareus et al., 2008). Consistently, our study also suggests that inhibiting NF-κB signaling in the vasculature has antiatherogenic effects and may present a therapeutic strategy to treat atherosclerosis.

Unexpectedly, IKKβ-deficient mice were protected from diet-induced obesity and associated metabolic disorders. Recent studies have indicated that IKKβ–NF-κB signaling is involved in the development of obesity and associated metabolic disorders (Baker et al., 2011; Solinas and Karin, 2010). Diet-induced obesity and insulin resistance have been associated with the activation of IKKβ–NF-κB in multiple tissues including liver, adipose tissue, and brain (Yuan et al., 2001; Arkan et al., 2005; Cai et al., 2005; Zhang et al., 2008; Chiang et al., 2009; Jiao et al., 2011; Purkayastha et al., 2011). Heterozygous deletion of IKKβ or inhibiting IKKβ activity with salicylates protected mice against insulin resistance triggered by HF feeding or obesity (Kim et al., 2001; Yuan et al., 2001). Interestingly, deletion of IKKβ in skeletal muscle fails to prevent obesity-induced insulin resistance (Rohl et al., 2004). In the current study, we found that SM22Cre-mediated IKKβ deletion protected mice from HF feeding-induced vascular and systemic inflammation.
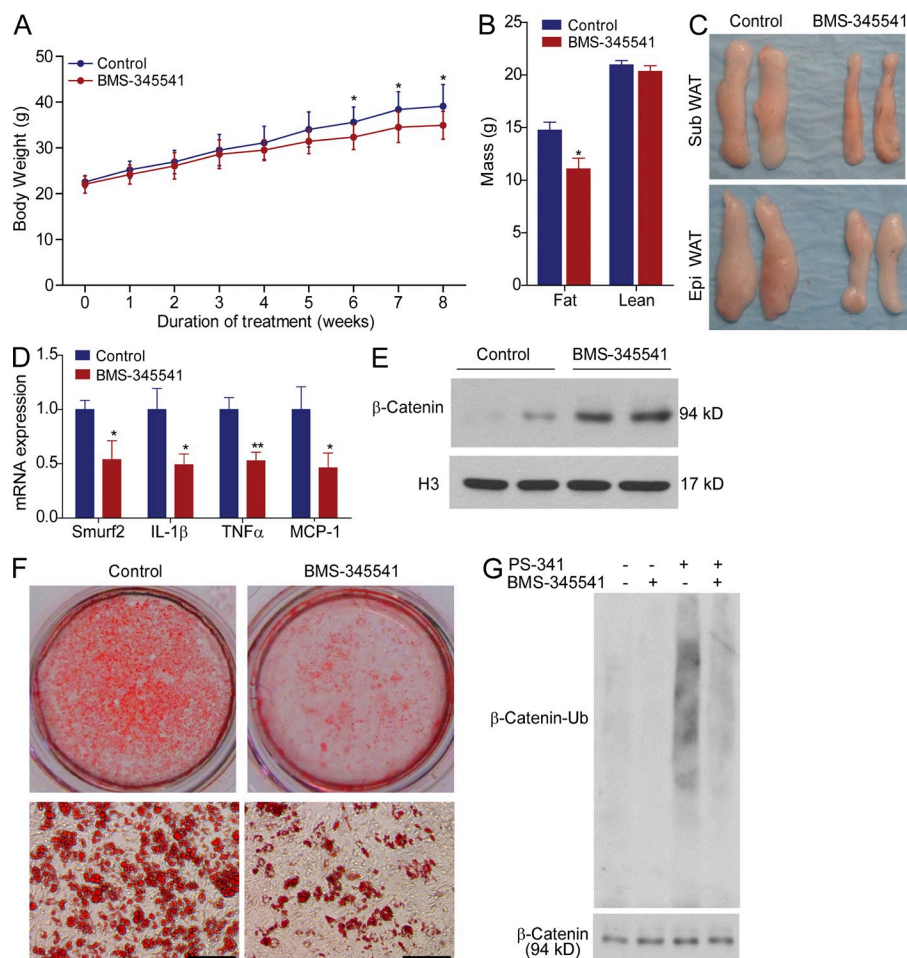
Figure 9. Chronic treatment of mice with IKKβ inhibitor ameliorates diet-induced obesity. (A and B) 8-wk-old male C57BL/6 mice were fed a WD and treated with vehicle or 10 mg/kg body weight of BMS-345541 by daily oral gavage for 8 wk. Body weight (A) was measured weekly and fat and lean mass (B) were measured at the end of feeding study (n = 11–12 mice). (C) Representative photographs of subcutaneous (Sub) and epididymal (Epi) WAT. (D) Expression of Smurf2 and other NF-κB target genes in WAT were analyzed by QPCR (n = 4 mice). (E) Western blot analysis of nuclear β-catenin levels in WAT of control or BMS-345541-treated mice. Nuclear proteins were probed with anti-Histone H3 antibodies an internal control. (F) Oil red O staining of adipose SV cells from control or BMS-345541–treated mice induced by differentiation medium. (G) Adipose SV cells isolated from control or BMS-345541-treated mice were incubated with vehicle or 100 nM PS-341 as indicated for 4 h. β-catenin was immunoprecipitated with anti–β-catenin antibodies and then probed with antiubiquitin monoclonal antibodies. The whole cell lysates were probed with anti–β-catenin antibodies as an internal control. Similar results were obtained from at least three independent experiments. All data are mean ± SD. *, P < 0.05; **, P < 0.01. Bars: (F, bottom) 100 µm.

In addition, IKKβ-deficient mice also had increased energy expenditure which may be partly explained by increased UCP-1 expression in WAT. Obesity is associated with chronic inflammation that plays a crucial role in the pathogenesis of insulin resistance and atherosclerosis (Gregor and Hotamisligil, 2011; Calay and Hotamisligil, 2013). While much attention has been focused on the activation of inflammatory cells in obesity, little is known about the contribution of vascular inflammation to the development of obesity and associated metabolic disorders. Our findings suggest that the vasculature may be one of the primary sites at which the inflammatory response occurs in obesity, and HF feeding-elicited vascular inflammation contributes to the development of obesity-associated metabolic disorders and atherosclerosis.

It is intriguing that SM22Cre-mediated IKKβ deletion protects mice from diet-induced adipose tissue growth. Blood vessels are present in virtually all organs and harbor mural cells (SMCs and pericytes), a heterogeneous class of cells that have been viewed as mesenchymal stem cells (MSCs) or multipotent progenitor cells capable to differentiate into adipocytes, chondrocytes, osteoblasts and myoblasts (Zeve et al., 2009). Tang et al. (Tang et al., 2008) used genetic marking, lineage tracing, and flow methodologies to identify a subset of mural cells as adipocyte progenitors. Adipocyte progenitors,

which reside in a vascular niche, express multiple SMC or pericyte markers including PDGFRβ, αSMA, and NG2 (Tang et al., 2008, 2011). An independent study by Friedman et al. (Rodeheffer et al., 2008) also isolated adipocyte progenitors with many similar features from adipose SV fraction. More recently, several other studies have confirmed these findings (Cai et al., 2011; Lee et al., 2012b; Berry and Rodeheffer, 2013). Our cell lineage analysis demonstrated the expression of SM22 in adipose SV cells, which is consistent with recent studies indicating that SM22Cre is active in perivascular adipocyte precursor cells (Olson and Soriano, 2011; Chang et al., 2012). For instance, Chang et al. (2012) reported that SM22Cre-mediated deletion of PPARγ caused an absence of perivascular fat, likely due to the deficiency of PPARγ in adipocyte precursor cells. Interestingly, we found that the adipogenic potential of IKKβ-deficient SV cells was markedly impaired. We also demonstrated that shRNA-mediated knockdown of IKKβ or pharmacological inhibition of IKKβ inhibits 3T3-L1 preadipocyte differentiation. Therefore, our results suggest that IKKβ functions in adipocyte precursor cells to regulate adipose tissue development.

Despite substantial progress in investigating preadipocyte differentiation, little is known about the initial signals that trigger adipocyte precursor cell differentiation in response to

consumption of a HF diet. It is noteworthy that IKKβ-deficient mice had normal adipose development when fed a chow diet but were protected from HF feeding–induced obesity. Nutrients are considered naturally inflammatory (Gregor and Hotamisligil, 2011), and overnutrition-mediated IKKβ activation may not only lead to the increased inflammatory responses in the vasculature but also initiate adipocyte precursor cell differentiation. In addition to mediating inflammatory responses, IKKβ–NF-κB signaling has been implicated in the regulation of hematopoietic cell development and stem cell differentiation (Sarkar et al., 2008; Vallabhapurapu and Karin, 2009; Gerondakis et al., 2012; Zhang et al., 2012; Chang et al., 2013). IKKβ-mediated NF-κB activation has been shown to be required for initial differentiation of neural stem cells (Zhang et al., 2012). Similar to our findings in adipose tissues, inhibition of IKKβ–NF-κB blocks neural stem cell differentiation and causes accumulation of neural stem cells in the brain (Zhang et al., 2012). Another study found that IKKβ–NF-κB pathway regulates osteogenic differentiation of MSCs by mediating β-catenin degradation (Chang et al., 2013). It has been observed that Wnt–β-catenin signaling inhibits adipogenesis in vitro and in vivo (Ross et al., 2000; Wright et al., 2007; Cristancho and Lazar, 2011). In the current study, we found that deficiency of IKKβ or inhibition of IKKβ activity blocked β-catenin ubiquitination and degradation in 3T3-L1 preadipocytes or adipose SV cells, resulting in elevated β-catenin levels and inhibited adipocyte differentiation. Because Wnt–β-catenin signaling positively regulates osteogenesis (Chang et al., 2013), it is plausible that overnutrition-mediated activation of IKKβ promotes adipogenic differentiation but blocks osteogenic differentiation of MSCs, which may contribute to the increased fat accumulation but decreased bone formation in diet-induced obesity. It would be interesting to further investigate how the crosstalk of NF-κB and Wnt signaling mediates adipogenesis and osteogenesis in response to HF feeding in the future.

Although our data suggest that IKKβ regulates adipogenesis through Wnt signaling, it is also possible that multiple mechanisms are involved in IKKβ-mediated adipocyte differentiation. For example, epigenetic mechanisms in particular histone modification also play an important role in regulating adipogenesis (Cho et al., 2009; Mikkelsen et al., 2010; Wang et al., 2013). In addition to β-catenin, Smurf2 mediates ubiquitination and degradation of the histone methyltransferase Ezh2 that regulates MSC differentiation (Wang et al., 2010; Yu et al., 2013). Furthermore, NF-κB can directly regulate transcription of several chromatin-modifying enzymes such as the H3K27 demethylase Jmjd3 (De Santa et al., 2007). NF-κB signaling has also been shown to epigenetically regulate the expression of transcription factors required for nuclear reprogramming (Lee et al., 2012a; O'Neill, 2012). Future studies will be required to determine whether NF-κB signaling can epigenetically regulate adipogenesis.

IKKβ inhibitors such as salicylates have been shown to ameliorate obesity-associated insulin resistance in animals and to exert beneficial effects in diabetic patients (Williamson, 1901;

Reid et al., 1957; Kim et al., 2001; Yuan et al., 2001). Interestingly, studies also indicate that long-term antiinflammatory therapy is associated with weight loss in humans (Boaz et al., 2009). We found that IKKβ inhibitors including salicylates and BMS-345541 efficiently inhibited 3T3-L1 cell differentiation in vitro and chronic treatment with BMS-345541 prevented diet-induced adiposity in mice. BMS-345541 treatment also decreased Smurf2 expression and stimulated the nuclear β-catenin accumulation in WAT. These in vivo results are consistent with previous studies showing that activation of Wnt signaling inhibits obesity in mice (Wright et al., 2007). Therefore, our studies provide evidence for the use of appropriate IKKβ inhibitors as a potential therapeutic strategy to treat obesity and metabolic disorders.

In summary, we have demonstrated an important role of IKKβ in the pathogenesis of obesity and atherosclerosis. Deficiency of IKKβ in SMCs decreased vascular inflammation and atherosclerosis development. Unexpectedly, IKKβ deficiency also protected mice from diet-induced obesity and associated metabolic disorders. Of particular interest is that ablation of IKKβ blocked adipocyte differentiation and induced accumulation of adipocyte precursor cells in WAT, suggesting that IKKβ functions as a regulator of adipocyte differentiation. Our results also raise the possibility that inhibition of IKKβ in the vasculature may present an innovative therapeutic strategy to treat obesity and atherosclerosis.

MATERIALS AND METHODS

Mice. SMC-specific IKKβ knockout (SM22Cre⁺IKKβ^F/F) mice were generated by crossing mice carrying loxP-flanked IKKβ alleles (IKKβ^F/F; Li et al., 2003) with SM22α-Cre (SM22Cre) transgenic mice (Holtwick et al., 2002). The mice used in this study were backcrossed at least seven additional generations onto the C57BL/6 background (>95% C57BL/6) using the marker-assisted Microsatellite Genotyping technique. To increase susceptibility to spontaneous atherosclerotic lesion development, the SM22Cre⁺ IKKβ^F/F mice were crossed with LDLR⁻/⁻ mice to generate SM22Cre⁺ IKKβ^F/F LDLR⁻/⁻ and IKKβ^F/F LDLR⁻/⁻ mice. The mice used in this study had IKKβ^F/F LDLR⁻/⁻ double mutant background and SM22Cre⁺IKKβ^F/F LDLR⁻/⁻ mice carried heterozygous knock-in for SM22Cre. For cell lineage analysis, SM22Cre mice were crossed with Rosa26^EGFP reporter mice (Mao et al., 2001) to generate SM22Cre⁺Rosa26^EGFP mice. For atherosclerosis studies, 4-wk-old male SM22Cre⁺IKKβ^F/F LDLR⁻/⁻ and IKKβ^F/F LDLR⁻/⁻ littermates were fed a standard chow diet, a HF WD (21.2% fat, 0.2% cholesterol; Harlan Teklad; Park et al., 2012), or a modified semisynthetic low-fat AIN76 diet (4.3% fat, 0.02% cholesterol; Research Diet; Teupser et al., 2003; Zhou et al., 2011) for 12 wk until euthanization at 16 wk of age. For IKKβ inhibitor treatment study, 8-wk-old WT male C57BL/6 mice (The Jackson Laboratory) were fed a WD and treated with vehicle (corn oil) or 10 mg/kg body weight BMS-345541 (Sigma-Aldrich) by daily oral gavage for 8 wk. All animals were housed in a specific pathogen–free environment with a light-dark cycle, under a protocol approved by the University of Kentucky Institutional Animal Care and Use Committee.

Metabolic measurements. Bodyweight was measured weekly and body composition was measured by NMR spectroscopy (Echo MRI) or dual-energy x-ray absorptiometry (DEXA; GE Healthcare Lunar). Food intake and oxygen consumption (VO_2) were measured for individually housed mice with a LabMaster system (TSE Systems) for 4–5 consecutively days. VO_2 data were normalized by lean body mass and average from 4-d measurements. Intraperitoneal glucose tolerance test (GTT) was performed as described previously (Zhou et al., 2011).

Blood analysis. Plasma total cholesterol and triglyceride concentrations were determined enzymatically by a colorimetric method (Zhou et al., 2011). Plasma from multiple mice ($n = 6$) was pooled and plasma lipoprotein cholesterol distributions were determined by fast-performance liquid chromatography (FPLC; Sui et al., 2011; Park et al., 2012). Plasma insulin was measured using a Rat/Mouse Insulin ELISA kit (Millipore). Plasma cytokine levels were determined by a mouse cytokine multiplex assay kit and a Bio-Plex 200 system (Bio-Rad Laboratories).

Atherosclerosis quantification. OCT-embedded hearts or brachiocephalic arteries were sectioned and stained with oil red O, and atherosclerotic lesions were quantified as described previously (Zhou et al., 2011; Park et al., 2012).

Vascular SMC isolation. Thoracic aortas were removed and the adventitia was gently removed. After removing ECs, SMCs were obtained by sequential digestion of the aortas with collagenase type II (175 U/ml) followed by collagenase type II (175 U/ml) and elastase (0.5 mg/ml). Cells were cultured in DMEM and SMC lineage was confirmed by immunofluorescence staining for α–SMA (Sigma-Aldrich) in >99% of the cells.

Nuclear protein isolation and electrophoretic mobility shift assay (EMSA). Nuclear protein isolation and EMSA was performed as previously described (Zhou et al., 2004; Park et al., 2012). In brief, SMCs were treated with TNF (20 ng/ml) or vehicle for 30 min. Nuclear proteins were prepared by standard methods and aliquots were stored at −80°C until use (Zhou et al., 2004). Oligonucleotides containing consensus NF-κB (Promega) was end-labeled to a specific activity of 10^5 CPM with γ-[^{32}P]ATP (GE Healthcare) using T4-polynucleotide kinase (Promega), followed by purification on a Nick column (GE Healthcare). The DNA–protein binding reactions were performed as described previously (Zhou et al., 2004; Park et al., 2012). The binding complexes were subjected to electrophoresis in a 6% nondenaturing polyacrylamide gel containing 0.5 X TBE. The gels were dried and exposed to films.

SV cell isolation and differentiation. SV cells and adipocytes were isolated from subcutaneous WAT. The SV cells were used for cell counting, RNA isolation, or culturing in 6-well plates for differentiation. For differentiation assays, SV cells were induced by high-glucose DMEM containing dexamethasone (1 μM), isobutylmethylxanthine (0.5 mM), insulin (10 μg/ml), and 10% FBS. 48 h after induction, the cells were maintained in high-glucose DMEM containing insulin (10 μg/ml) and 10% FBS till they were ready for analysis (Gupta et al., 2010). For flow cytometry analysis, SV cells were resuspended in ice-cold HBSS supplemented with 1.0% BSA and labeled with PE-CD31 (BD), PDGFRβ-biotin (eBioscience), or NG2 (Millipore) antibodies for 15 min on ice. Cells were then washed and resuspended in HBSS with 1.0% BSA followed by incubation with Alexa Fluor 647 streptavidin and Alexa Fluor 488 secondary antibodies (Life Technology) for 15 min on ice. Cells were then washed and resuspended in PBS with 1.0% BSA for the analysis. Flow cytometry was performed on a BD FACSCalibur flow cytometer. For data analysis, cells were initially selected by size, on the basis of forward scatter (FSC) and side scatter (SSC). Selected individual cells were further grouped by the presence of CD31, NG2, or PDGFRβ cell surface markers (Fig. S1).

RNA isolation and QPCR analysis. Total RNA was isolated from mouse tissues or cells using TRIzol Reagent (Life Technologies), and QPCR was performed using gene-specific primers and the SYBR Green PCR kit (Life Technologies) as previously described (Sui et al., 2011; Zhou et al., 2011). The sequences of primer sets used in this study are listed in Table S1.

3T3–L1 shRNA knockdown and differentiation. 3T3–L1 cells were obtained from ATCC. Short hairpin RNA (shRNA) plasmids targeting the mouse IKKβ gene sequence were provided in the lentivirus plasmid vector pLKO.1-Puro by Sigma-Aldrich. Lentivirus production and transduction of target cells were performed according to the manufacturer-supplied protocol. To express IκBαM in 3T3–L1 cells, IκBαM expression vector, which contains a serine to alanine mutation in amino acid 32 and 36 (Zhou et al., 2006), and control vector were transfected into 3T3–L1 cells using Amaxa Cell Line Nucleofector kit V (Lonza). For IKKβ inhibitor treatment, the cells were treated with BMS-345541 or sodium salicylate (Sigma-Aldrich) as indicated in the figure legends. For adipocyte differentiation assays, confluent 3T3–L1 cells were exposed to differentiation media (high-glucose DMEM supplemented with 10% FBS and differentiation cocktail including 1 μg/ml insulin, 1 μM dexamethasone, and 0.5 mM isobutylmethylxanthine). 48 h after induction, the cells were maintained in high-glucose DMEM containing insulin (1 μg/ml) and 10% FBS till they were ready for analysis.

Western blot analysis. Western blot analysis was performed as previously described (Park et al., 2012). Proteins were isolated from cells or mouse tissues by homogenization in RIPA buffer with complete mini protease inhibitor cocktail (Roche). Protein concentrations were determined by the Pierce BCA protein assay kit (Thermo Fisher Scientific). Anti-IKKβ, anti-IKKα, anti-Smurf2, and anti-Histone H3 antibodies were purchased from Cell Signaling Technology; anti–β-catenin, anti–β-actin, and anti-GAPDH antibodies were purchased from Sigma-Aldrich; and antiubiquitin monoclonal antibody was purchased from Santa Cruz Biotechnology. For immunoprecipitation experiments, control or shIKKβ 3T3–L1 cells, or adipose SV cells were incubated with 100 nM of PS-341 for 4 h. The whole-cell lysates were isolated, incubated with anti–β-catenin antibody overnight at 4°C, and then incubated with Protein A Agarose beads (Roche) for another 5 h. The samples were washed and analyzed by Western blot using antiubiquitin monoclonal antibodies.

Immunostaining. Immunocytochemistry was performed on cultured vascular SMCs to measure p65 translocation (Park et al., 2012). In brief, SMCs harvested from SM22Cre⁺IKKβ^F/F^LDLR^−/−^ mice and the control littermates were cultured in 8-chamber slides and treated with 20 ng/ml of TNF or vehicle for 30 min. Cells were then fixed with 100% acetone. Followed by washing with PBS, the cells were blocked with 10% normal rabbit sera, probed with rabbit anti–mouse p65 antibody (Abcam), and then detected with fluorescein-labeled secondary antibody. Immunohistochemical staining of atherosclerotic lesions and WAT were performed on 12-μm sections of heart roots or 10-μm sections of subcutaneous WAT freshly embedded in OCT (Zhou et al., 2011; Park et al., 2012). Sections were first fixed in 100% ice-cold acetone for 15 min and then washed with PBS for 20 min. Sections were permeabilized with PBS + 0.1% Triton X-100 (PBST) for 10 min. Nonspecific binding was reduced by incubating slides in 10% rabbit sera diluted in PBST for 20 min at room temperature. Sections were then incubated with antibodies against mouse MCP-1(Abcam), TNF (Abcam), IL-1β (Abcam), PDGFRβ (eBioscience), or Pref-1 (Abcam) at 4°C for 12–15 h. Sections were rinsed with PBS and incubated with fluorescein-labeled secondary antibodies (Life Technologies). The nuclei were stained by mounting the slides with DAPI medium (Vector Laboratories). Images were acquired with a Nikon fluorescence microscopy (Nikon). For immunohistochemical staining of adipose tissue macrophages, rehydrated antigen-retrieved sections were incubated with F4/80 (ABD Serotec) antiserum and visualized by the avidin–biotin complex method using the chromogen diaminobenzidine (Vector Laboratories).

Statistical analysis. All data are presented as the mean ± SD. Individual pairwise comparisons were analyzed by two-sample, two-tailed Student's t test for data normally distributed and by Mann-Whitney test for data not normally distributed, in which $P < 0.05$ was regarded as significant. n numbers are listed in figure legends or shown by scatter points.

Online supplemental material. Table S1 shows the sequences of primer sets used in this study. Fig. S1 shows flow cytometry gating strategies used for analyzing adipose SV cells. Online supplemental material is available at http://www.jem.org/cgi/content/full/jem.20131281/DC1.

REFERENCES

Arkan, M.C., A.L. Hevener, F.R. Greten, S. Maeda, Z.W. Li, J.M. Long, A. Wynshaw-Boris, G. Poli, J. Olefsky, and M. Karin. 2005. IKK-beta links inflammation to obesity-induced insulin resistance. *Nat. Med.* 11:191–198. http://dx.doi.org/10.1038/nm1185

Baker, R.G., M.S. Hayden, and S. Ghosh. 2011. NF-κB, inflammation, and metabolic disease. *Cell Metab.* 13:11–22. http://dx.doi.org/10.1016/j.cmet.2010.12.008

Berry, R., and M.S. Rodeheffer. 2013. Characterization of the adipocyte cellular lineage in vivo. *Nat. Cell Biol.* 15:302–308. http://dx.doi.org/10.1038/ncb2696

Boaz, M., L. Lisy, G. Zandman-Goddard, and J. Wainstein. 2009. The effect of anti-inflammatory (aspirin and/or statin) therapy on body weight in Type 2 diabetic individuals: EAT, a retrospective study. *Diabet. Med.* 26:708–713. http://dx.doi.org/10.1111/j.1464-5491.2009.02747.x

Brand, K., S. Page, G. Rogler, A. Bartsch, R. Brandl, R. Knuechel, M. Page, C. Kaltschmidt, P.A. Baeuerle, and D. Neumeier. 1996. Activated transcription factor nuclear factor-kappa B is present in the atherosclerotic lesion. *J. Clin. Invest.* 97:1715–1722. http://dx.doi.org/10.1172/JCI118598

Burke, J.R., M.A. Pattoli, K.R. Gregor, P.J. Brassil, J.F. MacMaster, K.W. McIntyre, X. Yang, V.S. Iotzova, W. Clarke, J. Strnad, et al. 2003. BMS-345541 is a highly selective inhibitor of I kappa B kinase that binds at an allosteric site of the enzyme and blocks NF-kappa B–dependent transcription in mice. *J. Biol. Chem.* 278:1450–1456. http://dx.doi.org/10.1074/jbc.M209677200

Cai, D., M. Yuan, D.F. Frantz, P.A. Melendez, L. Hansen, J. Lee, and S.E. Shoelson. 2005. Local and systemic insulin resistance resulting from hepatic activation of IKK-beta and NF-kappaB. *Nat. Med.* 11:183–190. http://dx.doi.org/10.1038/nm1166

Cai, X., Y. Lin, P.V. Hauschka, and B.E. Grottkau. 2011. Adipose stem cells originate from perivascular cells. *Biol. Cell.* 103:435–447. http://dx.doi.org/10.1042/BC20110033

Calay, E.S., and G.S. Hotamisligil. 2013. Turning off the inflammatory, but not the metabolic, flames. *Nat. Med.* 19:265–267. http://dx.doi.org/10.1038/nm.3114

Cawthorn, W.P., E.L. Scheller, and O.A. MacDougald. 2012. Adipose tissue stem cells meet preadipocyte commitment: going back to the future. *J. Lipid Res.* 53:227–246. http://dx.doi.org/10.1194/jlr.R021089

Chang, L., L. Villacorta, R. Li, M. Hamblin, W. Xu, C. Dou, J. Zhang, J. Wu, R. Zeng, and Y.E. Chen. 2012. Loss of perivascular adipose tissue on peroxisome proliferator-activated receptor-γ deletion in smooth muscle cells impairs intravascular thermoregulation and enhances atherosclerosis. *Circulation.* 126:1067–1078. http://dx.doi.org/10.1161/CIRCULATIONAHA.112.104489

Chang, J., F. Liu, M. Lee, B. Wu, K. Ting, J.N. Zara, C. Soo, K. Al Hezaimi, W. Zou, X. Chen, et al. 2013. NF-κB inhibits osteogenic differentiation of mesenchymal stem cells by promoting β-catenin degradation. *Proc. Natl. Acad. Sci. USA.* 110:9469–9474. http://dx.doi.org/10.1073/pnas.1300532110

Chiang, S.H., M. Bazuine, C.N. Lumeng, L.M. Geletka, J. Mowers, N.M. White, J.T. Ma, J. Zhou, N. Qi, D. Westcott, et al. 2009. The protein kinase IKKepsilon regulates energy balance in obese mice. *Cell.* 138:961–975. http://dx.doi.org/10.1016/j.cell.2009.06.046

Cho, Y.W., S. Hong, Q. Jin, L. Wang, J.E. Lee, O. Gavrilova, and K. Ge. 2009. Histone methylation regulator PTIP is required for PPARgamma and C/EBPalpha expression and adipogenesis. *Cell Metab.* 10:27–39. http://dx.doi.org/10.1016/j.cmet.2009.05.010

Cristancho, A.G., and M.A. Lazar. 2011. Forming functional fat: a growing understanding of adipocyte differentiation. *Nat. Rev. Mol. Cell Biol.* 12:722–734. http://dx.doi.org/10.1038/nrm3198

De Santa, F., M.G. Totaro, E. Prosperini, S. Notarbartolo, G. Testa, and G. Natoli. 2007. The histone H3 lysine-27 demethylase Jmjd3 links inflammation to inhibition of polycomb-mediated gene silencing. *Cell.* 130: 1083–1094. http://dx.doi.org/10.1016/j.cell.2007.08.019

Ferreira, V., K.W. van Dijk, A.K. Groen, R.M. Vos, J. van der Kaa, M.J. Gijbels, L.M. Havekes, and H. Pannekoek. 2007. Macrophage-specific inhibition of NF-kappaB activation reduces foam-cell formation. *Atherosclerosis.* 192: 283–290. http://dx.doi.org/10.1016/j.atherosclerosis.2006.07.018

Gareus, R., E. Kotsaki, S. Xanthoulea, I. van der Made, M.J. Gijbels, R. Kardakaris, A. Polykratis, G. Kollias, M.P. de Winther, and M. Pasparakis. 2008. Endothelial cell-specific NF-kappaB inhibition protects mice from atherosclerosis. *Cell Metab.* 8:372–383. http://dx.doi.org/10.1016/j.cmet.2008.08.016

Gerondakis, S., A. Banerjee, G. Grigoriadis, A. Vasanthakumar, R. Gugasyan, T. Sidwell, and R.J. Grumont. 2012. NF-κB subunit specificity in hemopoiesis. *Immunol. Rev.* 246:272–285. http://dx.doi.org/10.1111/j.1600-065X.2011.01090.x

Goossens, P., M.N. Vergouwe, M.J. Gijbels, D.M. Curfs, J.H. van Woezik, M.A. Hoeksema, S. Xanthoulea, P.J. Leenen, R.A. Rupec, M.H. Hofker, and M.P. de Winther. 2011. Myeloid IκBα deficiency promotes atherogenesis by enhancing leukocyte recruitment to the plaques. *PLoS ONE.* 6:e22327. http://dx.doi.org/10.1371/journal.pone.0022327

Gregor, M.F., and G.S. Hotamisligil. 2011. Inflammatory mechanisms in obesity. *Annu. Rev. Immunol.* 29:415–445. http://dx.doi.org/10.1146/annurev-immunol-031210-101322

Gupta, R.K., Z. Arany, P. Seale, R.J. Mepani, L. Ye, H.M. Conroe, Y.A. Roby, H. Kulaga, R.R. Reed, and B.M. Spiegelman. 2010. Transcriptional control of preadipocyte determination by Zfp423. *Nature.* 464:619–623. http://dx.doi.org/10.1038/nature08816

Gupta, R.K., R.J. Mepani, S. Kleiner, J.C. Lo, M.J. Khandekar, P. Cohen, A. Frontini, D.C. Bhowmick, L. Ye, S. Cinti, and B.M. Spiegelman. 2012. Zfp423 expression identifies committed preadipocytes and localizes to adipose endothelial and perivascular cells. *Cell Metab.* 15:230–239. http://dx.doi.org/10.1016/j.cmet.2012.01.010

Han, G., A.G. Li, Y.Y. Liang, P. Owens, W. He, S. Lu, Y. Yoshimatsu, D. Wang, P. Ten Dijke, X. Lin, and X.J. Wang. 2006. Smad7-induced beta-catenin degradation alters epidermal appendage development. *Dev. Cell.* 11:301–312. http://dx.doi.org/10.1016/j.devcel.2006.06.014

Hayden, M.S., and S. Ghosh. 2008. Shared principles in NF-kappaB signaling. *Cell.* 132:344–362. http://dx.doi.org/10.1016/j.cell.2008.01.020

Hideshima, T., P. Richardson, D. Chauhan, V.J. Palombella, P.J. Elliott, J. Adams, and K.C. Anderson. 2001. The proteasome inhibitor PS-341 inhibits growth, induces apoptosis, and overcomes drug resistance in human multiple myeloma cells. *Cancer Res.* 61:3071–3076.

Holtwick, R., M. Gotthardt, B. Skryabin, M. Steinmetz, R. Potthast, B. Zetsche, R.E. Hammer, J. Herz, and M. Kuhn. 2002. Smooth muscle-selective deletion of guanylyl cyclase-A prevents the acute but not chronic effects of ANP on blood pressure. *Proc. Natl. Acad. Sci. USA.* 99:7142–7147. http://dx.doi.org/10.1073/pnas.102650499

Hou, Y., F. Li, M. Karin, and M.C. Ostrowski. 2008. Analysis of the IKKbeta/NF-kappaB signaling pathway during embryonic angiogenesis. *Dev. Dyn.* 237:2926–2935. http://dx.doi.org/10.1002/dvdy.21723

Jiao, P., J. Ma, B. Feng, H. Zhang, J.A. Diehl, Y.E. Chin, W. Yan, and H. Xu. 2011. FFA-induced adipocyte inflammation and insulin resistance: involvement of ER stress and IKKβ pathways. *Obesity (Silver Spring).* 19:483–491. http://dx.doi.org/10.1038/oby.2010.200

Kanters, E., M. Pasparakis, M.J. Gijbels, M.N. Vergouwe, I. Partouns-Hendriks, R.J. Fijneman, B.E. Clausen, I. Förster, M.M. Kockx, K. Rajewsky, et al. 2003. Inhibition of NF-kappaB activation in macrophages increases atherosclerosis in LDL receptor–deficient mice. *J. Clin. Invest.* 112:1176–1185. http://dx.doi.org/10.1172/JCI200318580

Karin, M. 2006. Nuclear factor-kappaB in cancer development and progression. *Nature.* 441:431–436. http://dx.doi.org/10.1038/nature04870

Kim, J.K., Y.J. Kim, J.J. Fillmore, Y. Chen, I. Moore, J. Lee, M. Yuan, Z.W. Li, M. Karin, P. Perret, et al. 2001. Prevention of fat-induced insulin resistance by salicylate. *J. Clin. Invest*. 108:437–446. http://dx.doi.org/10.1172/JCI11559

Lancaster, G.I., B. Skiba, C. Yang, H.T. Nicholls, K.G. Langley, M.H. Chan, C.R. Bruce, G.W. Rewcastle, P.R. Shepherd, M. Karin, and M.A. Febbraio. 2012. IκB kinase β (IKKβ) does not mediate feedback inhibition of the insulin signalling cascade. *Biochem. J*. 442:723–732. http://dx.doi.org/10.1042/BJ20112037

Lee, J., N. Sayed, A. Hunter, K.F. Au, W.H. Wong, E.S. Mocarski, R.R. Pera, E. Yakubov, and J.P. Cooke. 2012a. Activation of innate immunity is required for efficient nuclear reprogramming. *Cell*. 151:547–558. http://dx.doi.org/10.1016/j.cell.2012.09.034

Lee, Y.H., A.P. Petkova, E.P. Mottillo, and J.G. Granneman. 2012b. In vivo identification of bipotential adipocyte progenitors recruited by β3-adrenoceptor activation and high-fat feeding. *Cell Metab*. 15:480–491. http://dx.doi.org/10.1016/j.cmet.2012.03.009

Li, Z.W., S.A. Omori, T. Labuda, M. Karin, and R.C. Rickert. 2003. IKK beta is required for peripheral B cell survival and proliferation. *J. Immunol*. 170:4630–4637.

Libby, P. 2002. Inflammation in atherosclerosis. *Nature*. 420:868–874. http://dx.doi.org/10.1038/nature01323

Mao, X., Y. Fujiwara, A. Chapdelaine, H. Yang, and S.H. Orkin. 2001. Activation of EGFP expression by Cre-mediated excision in a new ROSA26 reporter mouse strain. *Blood*. 97:324–326. http://dx.doi.org/10.1182/blood.V97.1.324

Melzner, I., V. Scott, K. Dorsch, P. Fischer, M. Wabitsch, S. Brüderlein, C. Hasel, and P. Möller. 2002. Leptin gene expression in human preadipocytes is switched on by maturation-induced demethylation of distinct CpGs in its proximal promoter. *J. Biol. Chem*. 277:45420–45427. http://dx.doi.org/10.1074/jbc.M208511200

Mikkelsen, T.S., Z. Xu, X. Zhang, L. Wang, J.M. Gimble, E.S. Lander, and E.D. Rosen. 2010. Comparative epigenomic analysis of murine and human adipogenesis. *Cell*. 143:156–169. http://dx.doi.org/10.1016/j.cell.2010.09.006

Millar, S.E. 2006. Smad7: licensed to kill beta-catenin. *Dev. Cell*. 11:274–276. http://dx.doi.org/10.1016/j.devcel.2006.08.008

Monaco, C., E. Andreakos, S. Kiriakidis, C. Mauri, C. Bicknell, B. Foxwell, N. Cheshire, E. Paleolog, and M. Feldmann. 2004. Canonical pathway of nuclear factor kappa B activation selectively regulates proinflammatory and prothrombotic responses in human atherosclerosis. *Proc. Natl. Acad. Sci. USA*. 101:5634–5639. http://dx.doi.org/10.1073/pnas.0401060101

Moore, K.J., and I. Tabas. 2011. Macrophages in the pathogenesis of atherosclerosis. *Cell*. 145:341–355. http://dx.doi.org/10.1016/j.cell.2011.04.005

O'Neill, L.A. 2012. "Transflammation": when innate immunity meets induced pluripotency. *Cell*. 151:471–473. http://dx.doi.org/10.1016/j.cell.2012.10.006

Olefsky, J.M., and C.K. Glass. 2010. Macrophages, inflammation, and insulin resistance. *Annu. Rev. Physiol*. 72:219–246. http://dx.doi.org/10.1146/annurev-physiol-021909-135846

Olson, L.E., and P. Soriano. 2011. PDGFRβ signaling regulates mural cell plasticity and inhibits fat development. *Dev. Cell*. 20:815–826. http://dx.doi.org/10.1016/j.devcel.2011.04.019

Park, S.H., Y. Sui, F. Gizard, J. Xu, J. Rios-Pilier, R.N. Helsley, S.S. Han, and C. Zhou. 2012. Myeloid-specific IκB kinase β deficiency decreases atherosclerosis in low-density lipoprotein receptor-deficient mice. *Arterioscler. Thromb. Vasc. Biol*. 32:2869–2876. http://dx.doi.org/10.1161/ATVBAHA.112.254573

Purkayastha, S., G. Zhang, and D. Cai. 2011. Uncoupling the mechanisms of obesity and hypertension by targeting hypothalamic IKK-β and NF-κB. *Nat. Med*. 17:883–887. http://dx.doi.org/10.1038/nm.2372

Reid, J., A.I. MacDougall, and M.M. Andrews. 1957. Aspirin and diabetes mellitus. *BMJ*. 2:1071–1074. http://dx.doi.org/10.1136/bmj.2.5053.1071

Rodeheffer, M.S., K. Birsoy, and J.M. Friedman. 2008. Identification of white adipocyte progenitor cells in vivo. *Cell*. 135:240–249. http://dx.doi.org/10.1016/j.cell.2008.09.036

Röhl, M., M. Pasparakis, S. Baudler, J. Baumgartl, D. Gautam, M. Huth, R. De Lorenzi, W. Krone, K. Rajewsky, and J.C. Brüning. 2004. Conditional disruption of IkappaB kinase 2 fails to prevent obesity-induced insulin resistance. *J. Clin. Invest*. 113:474–481. http://dx.doi.org/10.1172/JCI200418712

Ross, S.E., N. Hemati, K.A. Longo, C.N. Bennett, P.C. Lucas, R.L. Erickson, and O.A. MacDougald. 2000. Inhibition of adipogenesis by Wnt signaling. *Science*. 289:950–953. http://dx.doi.org/10.1126/science.289.5481.950

Sarkar, F.H., Y. Li, Z. Wang, and D. Kong. 2008. NF-kappaB signaling pathway and its therapeutic implications in human diseases. *Int. Rev. Immunol*. 27:293–319. http://dx.doi.org/10.1080/08830180802276179

Solinas, G., and M. Karin. 2010. JNK1 and IKKbeta: molecular links between obesity and metabolic dysfunction. *FASEB J*. 24:2596–2611. http://dx.doi.org/10.1096/fj.09-151340

Spalding, K.L., E. Arner, P.O. Westermark, S. Bernard, B.A. Buchholz, O. Bergmann, L. Blomqvist, J. Hoffstedt, E. Näslund, T. Britton, et al. 2008. Dynamics of fat cell turnover in humans. *Nature*. 453:783–787. http://dx.doi.org/10.1038/nature06902

Sui, Y., J. Xu, J. Rios-Pilier, and C. Zhou. 2011. Deficiency of PXR decreases atherosclerosis in apoE-deficient mice. *J. Lipid Res*. 52:1652–1659. http://dx.doi.org/10.1194/jlr.M017376

Tang, Q.Q., and M.D. Lane. 2012. Adipogenesis: from stem cell to adipocyte. *Annu. Rev. Biochem*. 81:715–736. http://dx.doi.org/10.1146/annurev-biochem-052110-115718

Tang, W., D. Zeve, J.M. Suh, D. Bosnakovski, M. Kyba, R.E. Hammer, M.D. Tallquist, and J.M. Graff. 2008. White fat progenitor cells reside in the adipose vasculature. *Science*. 322:583–586. http://dx.doi.org/10.1126/science.1156232

Tang, W., D. Zeve, J. Seo, A.Y. Jo, and J.M. Graff. 2011. Thiazolidinediones regulate adipose lineage dynamics. *Cell Metab*. 14:116–122. http://dx.doi.org/10.1016/j.cmet.2011.05.012

Teupser, D., A.D. Persky, and J.L. Breslow. 2003. Induction of atherosclerosis by low-fat, semisynthetic diets in LDL receptor-deficient C57BL/6J and FVB/NJ mice: comparison of lesions of the aortic root, brachiocephalic artery, and whole aorta (en face measurement). *Arterioscler. Thromb. Vasc. Biol*. 23:1907–1913. http://dx.doi.org/10.1161/01.ATV.0000090126.34881.B1

Vallabhapurapu, S., and M. Karin. 2009. Regulation and function of NF-kappaB transcription factors in the immune system. *Annu. Rev. Immunol*. 27:693–733. http://dx.doi.org/10.1146/annurev.immunol.021908.132641

Wang, L., Q. Jin, J.E. Lee, I.H. Su, and K. Ge. 2010. Histone H3K27 methyltransferase Ezh2 represses Wnt genes to facilitate adipogenesis. *Proc. Natl. Acad. Sci. USA*. 107:7317–7322. http://dx.doi.org/10.1073/pnas.1000031107

Wang, L., S. Xu, J.E. Lee, A. Baldridge, S. Grullon, W. Peng, and K. Ge. 2013. Histone H3K9 methyltransferase G9a represses PPARγ expression and adipogenesis. *EMBO J*. 32:45–59. http://dx.doi.org/10.1038/emboj.2012.306

Williamson, R.T. 1901. On the Treatment of Glycosuria and Diabetes Mellitus with Sodium Salicylate. *BMJ*. 1:760–762. http://dx.doi.org/10.1136/bmj.1.2100.760

Wolfrum, S., D. Teupser, M. Tan, K.Y. Chen, and J.L. Breslow. 2007. The protective effect of A20 on atherosclerosis in apolipoprotein E-deficient mice is associated with reduced expression of NF-kappaB target genes. *Proc. Natl. Acad. Sci. USA*. 104:18601–18606. http://dx.doi.org/10.1073/pnas.0709011104

Wright, W.S., K.A. Longo, V.W. Dolinsky, I. Gerin, S. Kang, C.N. Bennett, S.H. Chiang, T.C. Prestwich, C. Gress, C.F. Burant, et al. 2007. Wnt10b inhibits obesity in ob/ob and agouti mice. *Diabetes*. 56:295–303. http://dx.doi.org/10.2337/db06-1339

Yu, Y.L., R.H. Chou, W.C. Shyu, S.C. Hsieh, C.S. Wu, S.Y. Chiang, W.J. Chang, J.N. Chen, Y.J. Tseng, Y.H. Lin, et al. 2013. Smurf2-mediated degradation of EZH2 enhances neuron differentiation and improves functional recovery after ischaemic stroke. *EMBO Mol. Med*. 5:531–547. http://dx.doi.org/10.1002/emmm.201201783

Yuan, M., N. Konstantopoulos, J. Lee, L. Hansen, Z.W. Li, M. Karin, and S.E. Shoelson. 2001. Reversal of obesity- and diet-induced insulin resistance with salicylates or targeted disruption of Ikkbeta. *Science*. 293:1673–1677. http://dx.doi.org/10.1126/science.1061620

Zeve, D., W. Tang, and J. Graff. 2009. Fighting fat with fat: the expanding field of adipose stem cells. *Cell Stem Cell*. 5:472–481. http://dx.doi.org/10.1016/j.stem.2009.10.014

Zhang, X., G. Zhang, H. Zhang, M. Karin, H. Bai, and D. Cai. 2008. Hypothalamic IKKbeta/NF-kappaB and ER stress link overnutrition

to energy imbalance and obesity. *Cell.* 135:61–73. http://dx.doi.org/10.1016/j.cell.2008.07.043

Zhang, Y., J. Liu, S. Yao, F. Li, L. Xin, M. Lai, V. Bracchi-Ricard, H. Xu, W. Yen, W. Meng, et al. 2012. Nuclear factor kappa B signaling initiates early differentiation of neural stem cells. *Stem Cells.* 30:510–524. http://dx.doi.org/10.1002/stem.1006

Zhou, C., M.M. Tabb, A. Sadatrafiei, F. Grün, A. Sun, and B. Blumberg. 2004. Hyperforin, the active component of St. John's wort, induces IL-8 expression in human intestinal epithelial cells via a MAPK-dependent, NF-kappaB–independent pathway. *J. Clin. Immunol.* 24:623–636. http://dx.doi.org/10.1007/s10875-004-6248-z

Zhou, C., M.M. Tabb, E.L. Nelson, F. Grün, S. Verma, A. Sadatrafiei, M. Lin, S. Mallick, B.M. Forman, K.E. Thummel, and B. Blumberg. 2006. Mutual repression between steroid and xenobiotic receptor and NF-kappaB signaling pathways links xenobiotic metabolism and inflammation. *J. Clin. Invest.* 116:2280–2289. http://dx.doi.org/10.1172/JCI26283

Zhou, C., B. Pridgen, N. King, J. Xu, and J.L. Breslow. 2011. Hyperglycemic Ins2AkitaLdlr$^{-/-}$ mice show severely elevated lipid levels and increased atherosclerosis: a model of type 1 diabetic macrovascular disease. *J. Lipid Res.* 52:1483–1493. http://dx.doi.org/10.1194/jlr.M014092